NTNU
Norwegian University of Science and Technology
Department of Marine Technology

Master Thesis

| **Title:** | **Delivered:** |
|---|---|
| **High energy ship collisions with bottom supported offshore wind turbines**<br>*Analyse av høyenergi skipsstøt mot bunnfaste offshore vinkraftverk* | June 3, 2011 |
| | **Availability:**<br>Open |
| **Student:**<br>Henriette Flathaug Ramberg | **Number of pages:**<br>66+Appendices |

**Abstract:**

Offshore wind farming is an industry under development and involves challenges. The farms might be located close to ship trading routes. This increases the risk of ship-wind farm impact, causing economic losses, environmental pollution and human fatalities. The first part of this report describes various bottom supported wind farm technologies and presents a discussion of the risk picture considering oil spill due to this collision event. A review of relevant standards is enclosed.

The main part of this thesis considers finite element modelling and simulations of impact between a jacket supported wind turbine and a large oil tanker. The goal with these analyses is to study the possibility of achieving the Bundesamt für Seeschifffahrt und Hydrographie standard "Design of Offshore Wind Turbines", requiring minor oil spill due to ship-wind turbine collision involving ship kinetic energy larger than 500 MJ. The standard requires that a risk analysis is performed to demonstrate that either the collision energy is absorbed by the structures or that it results in collapse of the wind turbine without damage of the ship hull.

The wind turbine model is received from the company Virtual Prototyping. Geometric and load modifications are performed in order to obtain realistic results representative for the North Sea. The global response of the jacket is studied using the computer program USFOS. The ship is modelled drifting towards the corner of the jacket, hitting one leg. The ship is assumed to be rigid, not contributing to dissipate the collision energy. The contact between the structures is represented by a nonlinear spring. Different impact locations on the jacket are considered.

Both collapse due to overall deformation of the installation and local damage of the tower is studied. In addition, failure of the nacelle bolts is investigated in order to verify the possibility of the nacelle dropping on the deck, penetrating the cargo tanks.

| **Keywords:** | **Advisor:** |
|---|---|
| Offshore jacket wind turbine<br>Ship collision<br>Finite element analysis; USFOS | Professor Jørgen Amdahl |

Address:
NTNU
Department of Marine Technology
N-7491 Trondheim

Location
Marinteknisk Senter
O. Nielsens vei 10

Tel. +47 73 595501
Fax +47 73 595697

Master Thesis 2011
for
Stud. Techn. Henriette Flathaug Ramberg

**High energy ship collisions with bottom supported offshore wind turbines**

*Analyse av høyenergi skipsstøt mot bunnfaste offshore vinkraftverk*

Offshore wind turbines may be located close to ship traffic lanes and thus exposed to ship collision. According to the Bundesamt für Seeschifffahrt und Hydrographie; Standard for Design of Offshore Wind Turbines (2007) the turbine has to be checked for collision with a tanker of 160 000 dwt, corresponding to a displacement of 190 000 tons. The impact speed is 2 m/s, which gives a kinetic energy of more than 500 MJ for sideway drifting and added mass of 40 %. For comparison, the standard collision energy with offshore vessels on the Norwegian Continental shelf is only 14 MJ.

With such huge amount of energy, it is not possible to design the wind turbine to resist the tanker (if the turbine was designed strong enough, the tanker would have to suffer major damage).

The best option is likely to construct the turbine such that it collapses into the sea in the drift direction of the tanker, actually without stopping the tanker, thus preventing the nacelle from dropping down on the tanker – and hence – opening of cargo tanks and direct hits of sailors – is avoided. The collapse may either be induced by buckling, yielding of the support structure, or foundation failure, e.g. piles being pulled out of the soil on the tension side.

To achieve such a design may be challenging; Because of the large inertia the support structure will be subjected to significant compression on the hit side in the early stages of collision. How to avoid the negative influence of failures on the hit side of the support structure; e.g. local buckling of stiffened/unstiffened columns etc.?

The USFOS software is a versatile tool for the global analysis, possibly in combination with other shell FE codes for local analysis. The purpose of the present work is to investigate the possibility of achieving the design requirements of the BSH standard.

The following tasks should be addressed:

**1: Background**

Perform a brief review of potential location for bottom supported offshore wind turbines in Europe and present areas with large ship traffic. Present an overview of relevant support structures (monopile, concrete foundations, jacket supports etc). Literature review of studies related to assessment of the consequences of ship impact with respect to structural damage and environmental pollution. Perform a brief review of the risk picture with respect to ship size and collision energy. Review of the Standard for Design of Offshore Wind Turbines issued by the Bundesamt für Seeschifffahrt und Hydrographie (2007). Other relevant standards should be considered.

**2: Calculation model**

Establish a calculation model for the jacket, tower and nacelle including any thrust force representing the wind turbine. The ship-jacket force interaction may be modeled as a nonlinear spring with representative properties. The pile/soil interaction shall be modeled with available features in USFOS. Modeling of potential local buckling modes of the tower shall be considered. Establish failure criteria for fixation of the turbine to the tower.

**3: Case Study**

Perform static and dynamic analysis of selected support designs subjected of the ship impact. Conduct sensitivity studies where important parameters are varied.
Identify collapse patterns:

- Will the tower collapse away or over the ship?
- Will the tower suffer local buckling in this process?
- Will the turbine fixation fail, so that the turbine drops freely down on the ship deck?
- What is the likely consequence of a fall on the ship deck?

**4: Improved design**

For selected case(s) investigate whether the design of the tower support may be improved so as to ensure tower collapse away from the ship

**5: Conclusions and recommendations for further work**

Literature studies of specific topics relevant to the thesis work may be included.

The work scope may prove to be larger than initially anticipated. Subject to approval from the supervisors, topics may be deleted from the list above or reduced in extent.

In the thesis the candidate shall present his personal contribution to the resolution of problems within the scope of the thesis work.

Theories and conclusions should be based on mathematical derivations and/or logic reasoning identifying the various steps in the deduction.

The candidate should utilise the existing possibilities for obtaining relevant literature.

**Thesis format**

The thesis should be organised in a rational manner to give a clear exposition of results, assessments, and conclusions. The text should be brief and to the point, with a clear language. Telegraphic language should be avoided.

The thesis shall contain the following elements: A text defining the scope, preface, list of contents, summary, main body of thesis, conclusions with recommendations for further work, list of symbols and acronyms, references and (optional) appendices. All figures, tables and equations shall be numerated.

The supervisors may require that the candidate, in an early stage of the work, presents a written plan for the completion of the work. The plan should include a budget for the use of computer and laboratory resources which will be charged to the department. Overruns shall be reported to the supervisors.

The original contribution of the candidate and material taken from other sources shall be clearly defined. Work from other sources shall be properly referenced using an acknowledged referencing system.

The report shall be submitted in two copies:

- Signed by the candidate
- The text defining the scope included
- In bound volume(s)
- Drawings and/or computer prints which cannot be bound should be organised in a separate folder.
- The report shall also be submitted in pdf format along with essential input files for computer analysis, spreadsheets, Matlab files etc in digital format.

**Deadline: June 14, 2011**

Trondheim, January 17, 2011

Jørgen Amdahl
Proefessor

Contact person at Virtual Prototyping:
Tore Holmås

# Preface

This report is written by Henriette Flathaug Ramberg and represents the results conducted in the Master Thesis work in the Master of Science Degree at the Norwegian University of Science and Technology (NTNU) in the spring semester 2011. The assignment is written within the specialised field of Marine structural engineering at the Department of Marine Technology (IMT). The Master Thesis is the final product of the Master of Science Degree. It covers the workload of one semester and gives 30 credits.

The assignment is given by Virtual Prototyping. The work is carried out under supervision of Professor Jørgen Amdahl at IMT and Tore Holmås at Virtual Prototyping.

The report presents the results from nonlinear analyses of a large oil tanker colliding with an offshore jacket wind turbine. The goal with this research is to verify or invalidate the German requirements for design energy in case of this collision event. The possibility of the installation falling towards the ship deck is studied. All simulations are executed in the computer program USFOS. Enclosed in Appendix B is a CD containing a digital version of the report, USFOS input files, and Excel calculation files.

I want to thank Professor Jørgen Amdahl for giving me the opportunity to work with such an interesting topic. He has been very helpful and had a large participation during the whole process, which I am grateful for. In addition, I want to thank Tore Holmås for providing software support and verification towards the industry concerning modelling.

I also want to thank my family for supporting me during this process. Special thanks to my partner Andreas and brother Joakim for discussing different aspects with me.

Trondheim, June 3, 2011

Henriette Flathaug Ramberg

## Summary

Offshore wind energy is a largely growing industry. However, its development involves some new challenges. The wind farm locations might be close to ship trading routes. Complications can involve impact between the two structures, causing environmental pollution due to oil spill. Risk analysis concerning the collision event must be executed. Water depth limits the choice of wind farm location. Both bottom supported wind turbine technologies for shallow water and floating structures used in deeper water, exists. However, the bottom supported designs are most developed.

The main goal with this research is to verify or invalidate the Bundesamt für Seeschifffahrt und Hydrographie standard "Design of Offshore Wind Turbines", requiring minor environmental pollution due collision between a jacket supported wind turbine and a 160 000 dwt oil tanker with kinetic energy larger than 500 MJ. The standard requires that either the impact energy is absorbed by the structures or the impact results in collapse of the wind turbine without damaging the ship hull.

The calculation model is received from the company Virtual Prototyping, providing solutions for wind turbines. Geometry and loads are modified in order to obtain realistic results, representative for the environmental conditions in the North Sea. The oil tanker is modelled with 190 000 tons in loaded condition and 70 000 tons in ballast. The ship is drifting towards the corner of the jacket, hitting one leg. The ship is assumed to be rigid, not contributing to dissipate the collision energy. The ship-jacket contact is modelled as a nonlinear spring. Three different impact cases are studied; loaded ship hitting the jacket leg in a joint at 20 m depth and the leg between two joints at 12.5 m, as well as ship in ballast hitting a joint at 5 m depth. All analyses of the jacket response are executed using the computer program USFOS. When studying the possibility of achieving the requirements in "Design of Offshore Wind Turbines", ballast ship impact is not of concern as it involves minor oil spill. However, it is included to illustrate the consequences of this event.

The collapse of the installation is studied. The results show that the global response of the installation is failure in the drifting direction of the ship. This involves minor environmental pollution. The results are mainly caused due to a weak upper layer in the soil. Based on this, the soil is excluded from the analyses, in order to verify the failure pattern. However, this causes the tower falling towards the ship due to the 20 m depth impact. In this impact event, buckling of the opposite leg not is present, which in the other cases assists the installation collapsing away from the ship. This outcome indicates the importance of correct soil characteristics. On the other hand, the contact at 20 m depth might be at a lower level than normally expected for a ship impact.

Local buckling on the hit side of the tower due to large inertia is evaluated, due to the possibility of the buckling causing the nacelle penetrating the ship hull. This is studied numerically by scaling axial stress to 146 MPa, corresponding to hand calculations of the buckling strength. The dynamic analyses of the impact at 5 m depth and the inter-joint impact exceed this limit. In order to include local buckling in the FE model, the lower beam element in the tower is replaced by shell elements, allowing out-of-plane buckling. However, the results disprove the possibility of local buckling of the tower.

In addition, large inertia can cause failure of the nacelle fixation due to large accelerations. This can involve the nacelle dropping on the ship deck, penetrating the cargo tanks. The fixation criterion for the bolts securing the nacelle to the tower requires horizontal acceleration less than 1 G. This limit is

not exceeded in any of the analyses. Based on this, the nacelle dropping on the ship deck is not of concern.

Based on the structural and environmental assumptions made in this work, the standard “Design of Offshore Wind Turbines” is demonstrated to be achieved. Neither overall nor local deformation causing major damage on the ship hull is present. Environmental pollution is not considered a problem in case of a 160 000 dwt oil tanker drifting into an offshore wind farm consisting of jacket supported installations.

# Contents

# List of Figures

## List of Tables

# Nomenclature

- The meaning of the symbols is given when introduced in the report
- Sometimes the same symbol indicates different quantities
- Vectors and matrices are represented by bold letters

## Roman letters

| | | |
|---|---|---|
| $a$ | Acceleration | [m/s$^2$] |
| $A$ | Cross-sectional area | [m$^2$] |
| $C$ | Reduced buckling coefficient | [-] |
| $C_D$ | Drag coefficient | [-] |
| $C_M$ | Mass coefficient | [-] |
| $d$ | Increment | [-] |
| $E$ | Elastic modulus/Energy | [Pa]/[J] |
| $F$ | Force | [N] |
| $F_M$ | Mass force | [N] |
| $F_D$ | Drag force | [N] |
| $F^i$ | Inertia force | [N] |
| $F^d$ | Damping force | [N] |
| $F^r$ | Restoring force | [N] |
| $k$ | Stiffness | [N/m] |
| $l$ | Length | [m] |
| $m$ | Mass | [kg] |
| $M_e$ | Elastic bending moment | [Nm] |
| $M_p$ | Plastic bending moment | [Nm] |
| $N$ | Normal force | [N] |
| $r$ | Radius | [m] |
| $R$ | External load | [R] |
| $t$ | Thickness/Time | [m]/[s] |
| $T$ | Period | [s] |
| $v$ | Velocity | [m/s] |
| $W_e$ | Elastic section modulus | [m$^3$] |
| $W_p$ | Plastic section modulus | [m$^3$] |
| $Z$ | Curvature parameter | [-] |

## Greek letters

| | | |
|---|---|---|
| $\alpha$ | Cross-sectional shape factor | [-] |
| $\gamma_m$ | Material factor | [-] |
| $\varepsilon_{cr}$ | Critical strain | [-] |
| $\lambda_{eq}$ | Equivalent reduced slenderness ratio | [-] |
| $\nu$ | Poisson's ratio | [-] |
| $\xi$ | Buckling coefficient | [-] |
| $\rho$ | Buckling coefficient/Density | [-]/[kg/m$^3$] |
| $\sigma_b$ | Bending stress | [Pa] |
| $\sigma_{b,E}$ | Bending Euler stress | [Pa] |
| $\sigma_{des}$ | Design buckling strength | [Pa] |

| | | |
|---|---|---|
| $\sigma_{des,e}$ | Elastic buckling strength | [Pa] |
| $\sigma_E$ | Euler stress | [Pa] |
| $\sigma_{eq}$ | Equivalent stress | [Pa] |
| $\sigma_{eq,cr}$ | Critical equivalent stress | [Pa] |
| $\sigma_x$ | Axial stress | [Pa] |
| $\sigma_{x,E}$ | Axial Euler stress | [Pa] |
| $\sigma_Y$ | Yield stress | [Pa] |
| $\Psi$ | Buckling coefficient | [-] |
| $\omega$ | Frequency | [rad/s] |

## Abbreviations

| | |
|---|---|
| ALS | Accidental Limit State |
| BSH | Bundesamt für Seeschifffahrt und Hydrographie |
| BWEA | British Wind Energy Association |
| DNV | Det Norske Veritas |
| EEA | European Environment Agency |
| EWEA | European Wind Energy Association |
| FE(A) | Finite Element (Analysis) |
| IMO | International Maritime Organization |
| IMT | Department of Marine Technology |
| NPD | Norwegian Petroleum Directorate |
| NTNU | Norwegian University of Science and Technology |
| ULS | Ultimate Limit State, return period of $10^{-2}$ |

# Chapter

## 1. Introduction

The worlds demand for energy is increasing. As the oil and gas reserves are diminishing as well as focus on environmental pollution is important, renewable energy is needed. Offshore wind energy might be one of the solutions securing power in the future. The wind around Europe's coast can deliver enough power to serve Europe seven times (EWEA). Offshore wind industry is under rapid development. By offshore installation of wind farms, noise and visual conflicts are avoided. In addition, the wind conditions and power utilisation are better at sea as the surface roughness is lower compared to on land (Nielsen, 2006).

However, offshore wind farms also involve new challenges. Collision between a large oil tanker and a jacket supported offshore wind turbine is of concern. Faulty manoeuvring or machinery blackout might lead to consequences of economic loss, environmental pollution and human lives. Figure 1 illustrates this impact scenario. The wind turbine represents the model used in this research, while the 160 000 dwt tanker "Cap Diamant" with a beam of 53 m and approximately 15 m draught is illustrating the ship (www.MarineTraffic.com, 2011, www.jpfil.com).

Figure 1: Illustrating picture of ship-wind turbine impact

The offshore jacket wind turbine will experience large deformations during a ship collision. The ship is assumed unaffected by impact with the jacket part of the installation. However, due to the large inertia in the turbine, the nacelle might drop down on the ship deck and penetrate the cargo tanks. This might introduce large environmental pollution. The Bundesamt für Seeschifffahrt und Hydrographie (BSH) standard "Design of Offshore Wind Turbines" requires risk analysis of the impact including kinetic energy of more than 500 MJ. Comparing this with what Norwegian Petroleum Directorate describes as a standard collision event in the North Sea, a supply vessel of 5 000 tons results in only 14 MJ collision energy (NPD, 1985).

### 1.1 Scope of work

This report considers the outcome of a sideways collision between an oil tanker and a jacket wind turbine. The objective with this research is to investigate the possibility of achieving the BSH design requirements and whether the consequences of impact due to a tanker drifting sideways towards the

offshore wind farm might be fatal environmentally. The dynamics are studied through finite element analysis (FEA) by using the software USFOS.

## 1.2 Limitations

The model used in the case studies executed in this work includes beam theory. Beam theory does not account for dents and load redistribution, which prevents out-of-plane buckling. However, in order to identify whether the wind turbine collapse pattern suffer from local buckling in the tower, hand calculations are used to identify the design buckling strength in the tower. Axial stress plots are scaled according to this value and exceeding is investigating. In addition, local buckling is further studied in the sensitivity studies, by replacing the lower beam element in the tower with shell elements.

In order to verify the results obtained during this work, several sensitivity studies are executed. This study involves variation of important parameters. The effect is studied by comparing the results to the original case studies. A limitation with this validation process is that the parameters are varied one at a time. Variation in several quantities might affect the results differently. However, this is not considered in this work.

When modelling the impact, the ship is assumed rigid. This involves that the ship do not participate in the kinetic energy dissipation. In reality, both structures will be involved in this process. However, this would require more complex simulations.

## 1.3 Thesis structure

This report has the following organization. The background and motivation for the research performed in this work is given in Chapter 2. The chapter contains a description of offshore wind turbine technologies, the industry development and a review of relevant standards concerning ship-wind turbine collision. Chapter 3 describes the wind turbine model and the ship-jacket contact representation. The procedure of the static and dynamic analyses is described in Chapter 4 and the results are presented in Chapter 5. In Chapter 6, the results are evaluated through sensitivity studies. Conclusions and recommendations for further work are given in Chapter 7.

# Chapter

## 2. Background

This chapter describes different offshore wind farm technologies and challenges related to offshore development of wind energy generation. Previous and ongoing work related to ship-wind turbine collision is enclosed. In addition, relevant standards considering the topic of this work are reviewed.

### 2.1 Offshore wind turbines

Offshore wind turbines consist of a turbine and a support structure. The turbine includes a nacelle and rotor blades, while the support structure is divided into a tower and a substructure. The foundation is described as the part of the wind turbine that is below the mud level (BSH, 2007).

In order to be cost-effective, bottom supported wind farms must be placed in shallow water. Floating structures can be installed in deeper water. However, the solution is expensive and more technological investigation is needed before development. Today, most wind farms are located in water depths up to about 25 m (EEA, 2009). Considering fixed wind turbines, different technologies are relevant (OffshoreWind.net, 2009):

- Monopiles consisting of a steel pile supporting the turbine, used up to 30 m water depth.
- Gravity foundations with large steel or concrete structures resting on the seabed.
- Tripods used in water depths between 30 and 50 m.
- Jackets with substructures build up by truss work.

See Figure 2 for depth estimates for different substructures, including floating wind turbines (Bard, 2010). At the end of 2010, 65 % of the substructures were monopiles, 25 % gravity foundations and 8 % jacket support (EWEA, 2011a).

At deep water, the wind is stronger and steadier. However, the environmental action is larger and stronger support structures are needed. Jackets are well known structures and have the advantage to be basically unaffected by waves. The structure has low mass and the global stiffness is high, while the local stiffness is low. Compared to the other technologies given above, the truss work in jackets distributes impact loads during collision. This requires a larger amount of energy before collapse. Jacket wind farms have the possibility of operating in deeper water compared to other bottom supported solutions and are today considered the optimal option for offshore wind energy development.

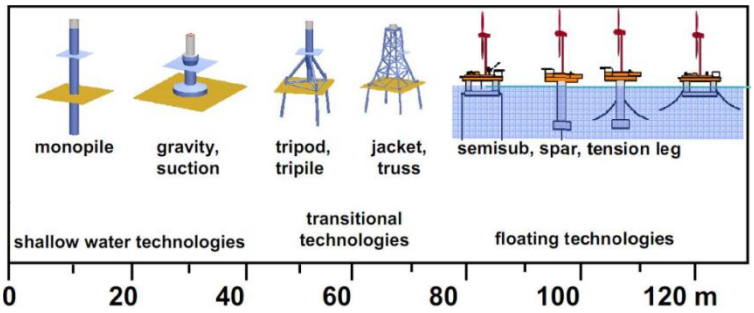


Figure 2: Platform technologies in varying depth

## 2.2 Offshore wind farm development

The United Kingdom and Norway have the largest available offshore area for wind energy generation (EEA, 2009). However, several factors limit the potential for development for offshore wind farms.

In order to study the possibility of bottom supported offshore wind farm installation, depth investigations of different locations is important. Figure 3 shows a bathymetry map over Europe (Bard, 2010). As seen, the possible locations for bottom supported offshore wind farms are mainly placed in Northern Europe, based on the depth limitations given in Figure 2.

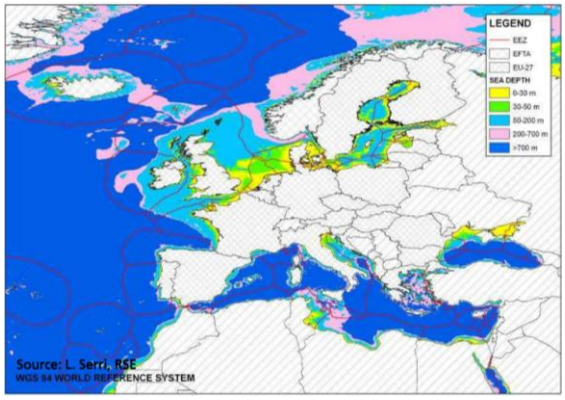


Figure 3: European bathymetry map

In addition to depth restrictions, studies of ship traffic lanes in and near the installation areas must be performed. Shipping routes are less concentrated in distances larger than 50 km from the coast (EEA, 2009). However, the depth increases with the distance from shore. The qualitative risk of a ship drifting into a wind turbine is defined as the probability of occurrence times the extent of the damage;

$$Risk = Probability * Consequence \quad (1)$$

Risk analysis shall be executed when evaluating offshore wind farm installation. The probability of collision is based on shipping traffic data. Automatic Identification System has been mandatory since December 31, 2004, and shall provide information about vessel traffic and navigation (IMO, 2004). The consequence of an impact between a ship and a fixed installation depends on the energy developed, which again depends on ship size and velocity (DNV, 2004, NORSOK, 2004b);

$$E = \frac{1}{2}(m+a)v^2 \quad (2)$$

where $E$ is the collision energy, $m$ and $a$ is the mass and added mass of the ship, respectively, and $v$ is the ship speed. Small fishing vessels might experience severe damage due to an impact with a bottom supported offshore wind turbine, while large oil tankers will possibly run down the installation without noticeable damage. The risk might be controlled by reducing the probability of ship collision by use of preventive and protective measures (Amdahl, 1991).

Today, Europe has offshore wind farms in nine countries (EWEA, 2011b). The distributed percentage of wind turbines is given in Figure 4. The two countries with the largest number of turbines as well as produced capacity are The United Kingdom and Denmark.

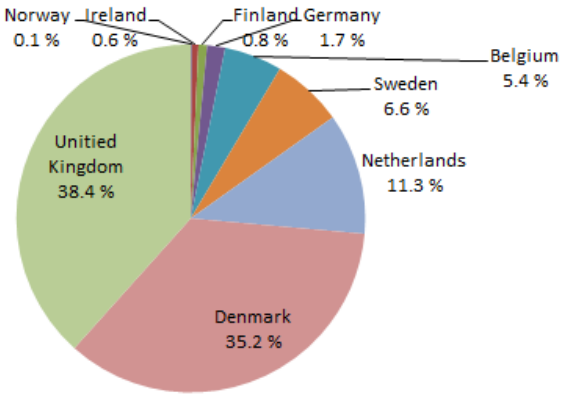


Figure 4: Operational offshore wind turbines in Europe at the end of 2010

## 2.3 Previous and ongoing related work

Several studies have been conducted within the ship-jacket collision event, mostly considering oil production jacket platforms. In that case, a robust jacket design is favourable (Amdahl and Johansen, 2001). However, considering impact between an oil tanker and a wind turbine, no major damage on the ship is desired. The best solution is to design the installation such that it collapses away from the ship due to the impact.

Biehl studied the consequences of a ship drifting into an offshore wind farm (Biehl, 2004). He considered impact between four different ship sizes with the different offshore wind turbine substructures described in Section 2.1. Considering the jacket, he concluded that there is a large variation of failure modes during collision, due to its large global and small local stiffness. His analyses stated that the turbine might fall in the direction of the ship.

Dalhoff and Biehl continued the study of collisions with wind farms (Dalhoff and Biehl, 2005). The purposed results are given in Table 1 with the matrix definitions in Table 2. As seen, impacts between large ships and jacket wind turbines are considered unsafe.

Table 1: Dalhoff and Biehl's results from collision simulations

| | | | | |
|---|---|---|---|---|
| Gravity based | $( )^1$ | $( )^1$ | $(\surd)^1$ | $( )^1$ |
| Steel tripod | $(\surd)^1$ | $(\surd)^1$ | $(\surd)^1$ | $(\surd)^1$ |
| Jacket | √ | √ | – | – |
| Mono pile | √ | √ | $\surd$ | $\surd$ |
| | Double hull<br>31 600 dwt | Container<br>2 300 TEU | Single hull<br>150 000 dwt | Bulk carrier<br>170 000 dwt |

Table 2: Dalhoff and Biehl's result matrix definitions

| | |
|---|---|
| √ | Calculation of collision scenarios did not show major hazards with this type of offshore wind turbine support structure and this vessel type. The design may be regarded as collision friendly for this vessel type. |
| (√) | Certain hazardous scenarios could be identified by numerical simulation. Countermeasures were given. The design may be regarded as conditionally collision friendly for this vessel type. |
| – | Hazardous scenarios were identified and no practicable countermeasures have been developed yet. So far, the design has to be considered unsafe. |
| | Not enough investigations have been made to verify the given results. |
| )[1] | See 5.2 for tripod and 5.4 for gravity based foundation. |

Biehl claimed that further investigations are needed regarding the possibility of the nacelle falling onto the ship and penetrating the hull with an oil spill as an outcome (Biehl, 2004). In 2007, Biehl and Lehmann studied a 5 MW turbine of 450 tons falling onto the ship deck with a speed of 35 m/s (Biehl and Lehmann, 2007). This corresponds to kinetic impact energy of 275 MJ. The conclusion was that if the nacelle drops at the center of the tank, it would penetrate the ship all the way from the deck to the outer bottom of the ship, causing environmental pollution. However, by disregarding the viscosity of the cargo in the analyses, this is a conservative estimate and might not represent the reality.

## 2.4 Relevant standards

SSPA Sweden AB conducted a project founded by Vattenfall and the Swedish Energy Agency with goal to develop a general approach for risk calculation of offshore wind farms, concerning ship traffic (Ellis et al., 2008). They stated that countries operate with different standards and purposed to develop an international guideline. This section compares the German requirements for offshore wind farms with the Norwegian standards.

The standard "Design of Offshore Wind Turbines" issued by BSH intends "to provide legal and planning security for development, design, implementation, operation and decommissioning of offshore wind farms" (BSH, 2007). It states that in case of a ship colliding with an offshore wind turbine, the ship shall be damaged as little as possible. The standard requires that extreme loads on the wind turbine, for example collision with ship, are calculated including partial safety factors in order to satisfy guidelines for stability against collapse.

In Annex 1; "Hull-retaining configuration of the substructure", it is stated that risk analysis of collisions is required. See Section 2.2 for definition of quantitative risk. According to the standard, the analysis should demonstrate that no major environmental pollution is a consequence because

a) either the entire collision energy can be absorbed by the ship and the offshore wind farm structure or
b) the offshore wind farm fails during the collision procedure without ripping open the ship's hull".

If this is satisfied, the wind turbine is called "collision friendly" and environmental pollution is minimal.

BSH demands the wind turbine to be modelled 5 m above the deck height of the ship. Masses and inertias above this level shall be included. The soil shall at least be applied as an elastic spring. The ship used in the analysis is a 160 000 dwt single-hulled tanker, corresponding to a displacement of 190 000

tons, unless data on shipping movements prove that this size of ship cannot reach the wind farm. The impact calculations shall be derived based on that the ship is drifting sideways into the wind turbine with a speed of 2 m/s, with no propulsion and thereby zero longitudinal speed. According to Equation 2, this results in a kinetic energy of more than 500 MJ, when assuming an added mass of 40 %;

$$E = \frac{1}{2}(190 \cdot 1.4)2^2 = 532\ MJ \tag{3}$$

Det Norske Veritas (DNV) states their requirements for ship impacts and collisions in the standard "Design of offshore wind turbine structures" (DNV, 2007). According to DNV, such accident shall be considered with ultimate limit state (ULS) analysis considering the ship as a variable functional load with partial safety factor of 1. Wind, waves and current shall be included in the analysis, in addition to the added mass contributing to kinetic energy. ULS design corresponds to the maximum load carrying capacity and the impact "load shall be taken as the largest unintended impact load in normal service conditions". The standard requires that neither the support structure nor the foundation suffer from damage. However, compared to the BSH standard, no specific ship size and impact energy requirement is given.

DNVs Recommended Practice c204 "Design Against Accidental Loads" describes collision analysis (DNV, 2004). The analysis is divided into two steps; external and internal collision mechanics. External mechanics is described as the amount of kinetic energy dissipated as strain energy, while internal mechanics is energy dissipated in the colliding structures. Three design principles are described in c204; strength, ductile and shared-energy design, see Figure 5. Considering tanker-wind turbine collision, one can expect ductile design. This implies that the ship is strong and resists the force with minor deformation, while the jacket undergoes large deformations and dissipates the energy.

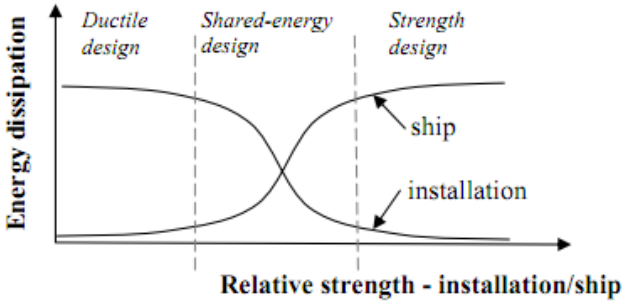


Figure 5: Design principles for energy dissipation

The NORSOK standard N-004 "Design of steel structures" requires non-linear dynamic finite element analyses or energy considerations combined with simple elastic-plastic methods for studying the effect of ship collision (NORSOK, 2004b). Interaction between three levels of strain energy dissipation is to be considered:

- Local cross-section
- Component/Sub-structure
- Total system

The dissipation is estimated from force-deformation relationships for the installation and the ship. However, N-004 only contains relationships for a supply vessel with a displacement of 5 000 tons.

Based on the review of the different regulations, the need for an international guideline as emphasized by SSPA Sweden AB is present.

# Chapter

## 3. Calculation model

This chapter focuses on establishing a representative offshore wind turbine model, sustainable to be used in the North Sea. It shall satisfy the standard requirements with an environmental factor of 1.3 and material factor of 1.15, resulting in a safety factor of 1.5. The chapter also includes a description of the ship modelling. The ship is assumed drifting sideways towards the wind turbine, hitting one of the legs. Three different impact cases is described in order to account for variation in water level, ship size and strength in jacket structure; a loaded ship hitting the jacket leg in a joint at 20 m below the sea surface, a ship in ballast hitting a joint at 5 m depth and a loaded ship hitting the leg between the two joints.

### 3.1 Software

The impact analysis is executed using USFOS; a computer program based on Lagrangian formulation for both static and dynamic analyses of frame structures (Amdahl et al.). USFOS is used to study resistance against accidental action and structures in damaged situation. Xact, USFOS Graphical User Interface, prepares and starts the analysis, USFOS Analysis Control executes the calculations and at last the results are presented in Xact. The fundamental concept of USFOS is to use one finite element for each physical element, using the same FE discretization as linear-elastic analysis (USFOS, 2001). Nonlinear material is modelled by use of plastic hinges. The elastic stiffness matrix is multiplied with the Livesly's stability functions, representing the axial force normalized to the Euler buckling force (Amdahl and Eberg, 1993).

### 3.2 Offshore wind turbine model

The calculation system is based on a USFOS model received from Virtual Prototyping, a company providing solutions for wind turbines (Virtual Prototyping). The model is described in the following.

#### 3.2.1 Model description

The USFOS input files are divided in three; head, model, and soil file. The head file contains the analysis commands, the model file describes the part of the model above the seabed, while the soil file describes the piles and soil condition. The system consists of the following parts; water, tower, jacket, piles and soil.

Gravity is included for the whole FE model. Buoyancy is included in the dynamic analyses, but neglected in the static analyses. The model consists of nodes connecting rectangular two-node, three-dimensional beam elements, with the option NODE and BEAM. All elements in the FE model are given pipe formed cross-section, with the option PIPE, except the foundation on top of the jacket, described below. The MISOIEP function defines all parts with elasto-plastic material and beam-column elements, see Figure 6 for material behavior (NORSOK, 2007). The model includes beam theory, which is based on the following assumptions (Moan, 2003):

- Hook`s law
- First order theory
- Navier`s hypothesis
- Neglecting stresses normal to the axes
- St. Venant`s theory

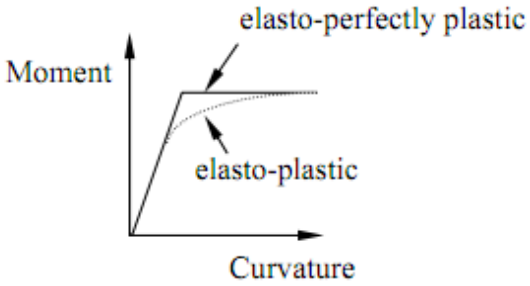


Figure 6: Elasto-plastic material

The part data described in the following is summarized in Table 3. The thickness variation in the tower is given in Figure 7.

Table 3: Model part data

| Part | Elastic-modulus | Poisson ratio | Yield strength | Density | Thermal expansion ratio | Length/ Height | Diameter/ Width | Thickness |
|---|---|---|---|---|---|---|---|---|
| Dimension | [MPa] | [-] | [MPa] | [kg/m$^3$] | [-] | [m] | [m] | [mm] |
| Tower | Sec. 3.2.2 | 0.3 | 350 | 7850 | - | 62 | 4-6 | 30 |
| Foundation | 2.1E5 | 0.3 | 440 | 7850 | 1.2E-5 | 3.5 | 2 | 50 |
| Jacket | 2.1E5 | 0.3 | Sec. 3.2.2 | 7850 | 1.2E-5 | 61.5 | 0.6-1.8 | 20-45 |
| Seabed | 2.1E5 | 0.3 | 400 | 0 | 0 | - | 120 | 1 |
| Piles | 2.1E5 | 0.3 | Sec. 3.2.2 | 7850 | 1.2E-5 | 69 | 1 | Sec. 3.2.2 |

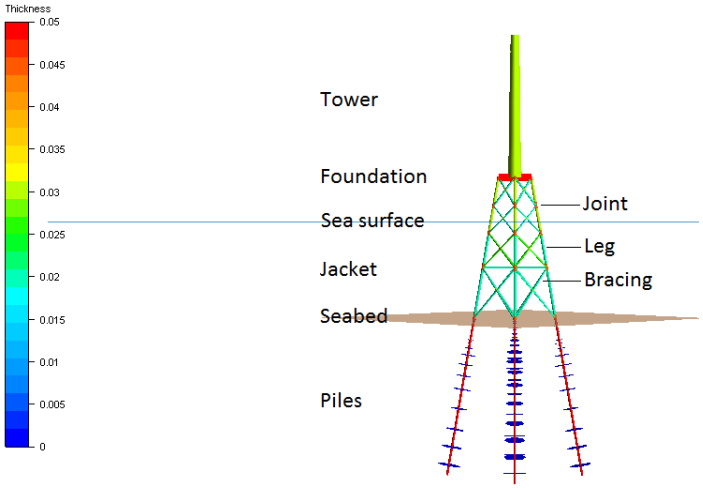


Figure 7: Wind turbine model thickness variation

The tower is 62 m high and 30 mm thick, see Figure 7. The diameter is increasing from 4 m at the top to 6 m at the jacket. The elastic modulus of the tower is discussed in Section 3.2.3. Poisson's ratio is 0.3, yield strength is 350 MPa, and density is 7850 kg/m$^3$. The part is shown in Figure 8.

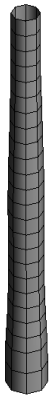

Figure 8: Tower model

The jacket consists of four levels and is 61.5 m high, see Figure 9. The diameter and thickness of the pipe elements varies between 0.6 to 1.8 m and 20 and 45 mm, respectively, depending on vertical location and whether the element is a column, joint or bracing. The thickness variation is shown in Figure 7. The yield strength of the jacket is described in Section 3.2.2. The elastic modulus is 2.1E5 MPa, Poisson's ratio is 0.3, and density is 7850 kg/m$^3$. The material is temperature dependent with a thermal expansion ratio of 1.2E-5. The four lowest nodes placed at the seabed are prevented from translation by including the boundary code "1 1 1 0 0 0".

The foundation connecting the tower to the jacket consists of four box elements, modelled with the option BOX. They are 3.5 m high, 2 m wide and have a thickness of 50 mm, see Figure 7. The foundation is made of the same material as the jacket, except the yield strength which is 440 MPa. The foundation is shown in Figure 9.

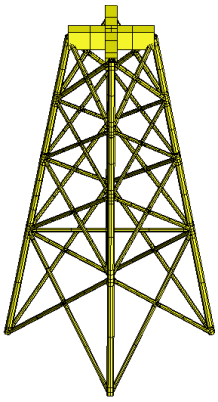

Figure 9: Jacket and foundation model

The seabed is defined as a 1 mm thick and 120 m wide square plate with the option MEMBRANE. It is fixed in the corners in all directions with "1 1 1 1 1 1" as boundary code. Elastic modulus is 2.1E5 MPa, Poisson's ratio is 0.3 and yield strength is 400 MPa. The density and thermal expansion is set to zero.

Including the soil file in the analysis, the translation prevention of the jacket is removed. This is done with the option CHG_BOUN, which redefines boundary conditions. The structure is connected to the seabed through plastic springs with the option SPRI_MOD, defining nonlinear soil characteristics without step scaling. The soil mainly consists of stiff clay, including soft clay from 1.8 to 12 m into the soil and two layers of sand at 18.6 and 36.2 m soil depth extending 4.5 and 16.8 m, respectively. The soil layers are shown in Figure 10. The loading is static. For more information about the soil characteristics, see the enclosed soil input files in Appendix B and USFOS User Manual (USFOS, 2010).

The piles are extending 69 m below the seabed into the soil, shown in Figure 10. They are fastened inside the jacket legs with an outer diameter of 1 m. The thickness and material yield strength of the piles is discussed in Section 3.2.2. Elastic modulus is 2.1E5 MPa, Poisson's ratio is 0.3, density is 7850 kg/m$^3$, and thermal expansion ratio is 1.2E-5.

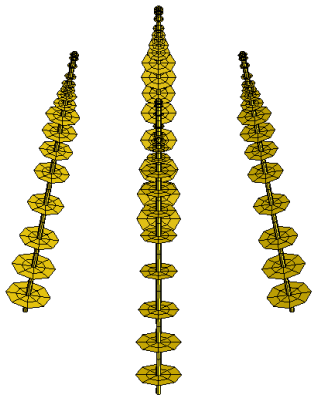

Figure 10: Soil and piles model

Both operating and closed down condition is studied when validating the model. During operation, wind passes the blades and makes them rotate. This creates a horizontal thrust force acting in the wind direction on top of the tower, representing the energy production. In the FE model this is included by the option NODELOAD. The nacelle is not modelled, but is included as a mass acting in top of the tower, with the option NODEMASS. As the blades are assumed to have little influence on the collapse of the wind turbine, which is the focus in this report, they are excluded from the analyses. During a storm, the production is closed down and there is no thrust force. The transition zone between these situations is approximately given as a wind speed of 25 m/s, see Figure 11 describing the operational limits (BWEA, 2005).

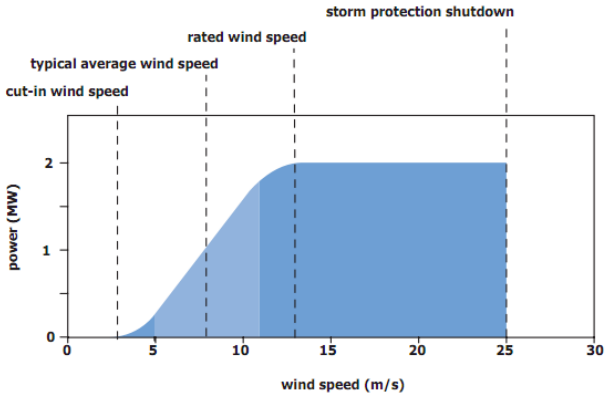


Figure 11: Typical power curve for a wind turbine

In addition to global and local damage of the wind turbine, the possibility of the nacelle breaking off the tower and dropping on the ship deck is studied. The failure criterion for the bolts fixing the nacelle to the tower is given by the horizontal acceleration in top of the tower. The critical acceleration is given as 1 G (Virtual Prototyping). If this limit is exceeded, the bolts will fail and direction of the dropping nacelle should be examined.

### 3.2.2 Model modifications

Some modifications are done with the original model in order to obtain a realistic solution and to withstand the North Sea environmental conditions. This section presents the changes carried out with the original model.

- The original wind turbine model contains horizontal bracings at the seabed. These are removed in order to make the model more realistic. The bracings can be seen in Figure 20 and Figure 21.
- The jacket and pile yield strength is reduced from 420 and 430 MPa, respectively, to 355 MPa which is a more realistic value.
- The model is given geometric imperfections with the size of 1.5 ‰ of the characteristic length with the option CINIDEF. In order to activate the imperfections, a dummy node load not acting normal or parallel to any of the model elements is included with the NODELOAD function of 1 N in all three directions in a random node. See Figure 12 for the effect of geometric imperfections on buckling strength, where P is force and w is curvature (Søreide, 1981). Figure 13 visualize the model imperfections scaled with a factor of 100. As seen, imperfection in each tower element is also shown.

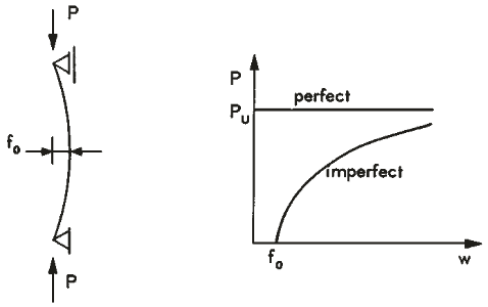


Figure 12: Effect of imperfections on buckling strength

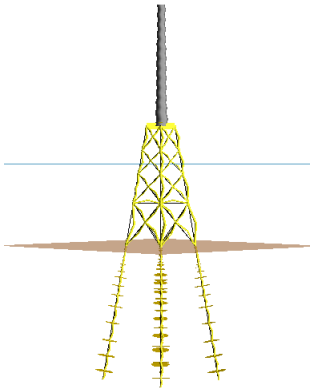

Figure 13: Wind turbine model imperfections

- Hydrodynamic forces are applied by including a dummy wave with 1 mm wave height, with the option WAVEDATA. Marine growth thickness, mass and drag coefficients are given according Table 4 by use of the options M_GROWTH, HYDRO_CD and HYDRO_CM. The values are interpolated between the given points and extrapolated outside. Marine growth affects the diameter of the jacket cylinders and affects the force calculation. The incremental force, $dF$, contribution from the mass-, $dF_M$, and drag forces, $dF_D$, is given by Morison's equation (Morison et al., 1950);

$$dF = dF_M + dF_D = \rho\pi\frac{D^2}{4}C_M a + \frac{\rho}{2}C_D|v|v \tag{4}$$

where $\rho$ is the fluid density, $D$ is the cylinder diameter and $a$ and $v$ is the fluid acceleration and velocity, respectively. $C_M$ and $C_D$ are the mass and drag coefficients, respectively.

Table 4: Hydrodynamic forces

| z-coordinate [m] | Marine growth thickness [m] | Drag coefficient [-] | Mass coefficient [-] |
|---|---|---|---|
| 5 | - | 0.65 | 1.6 |
| 0 | 0.08 | 0.65 | 1.6 |
| -5 | 0.06 | 1.05 | 1.2 |
| -12 | 0.04 | - | - |
| -42 | - | 1.05 | 1.2 |
| -120 | 0.00 | - | - |

- The water depth is increased from its original 30 to 42 m in the WAVEDATA option.
- Linear damping of the system is given by Rayleigh damping, RAYLDAMP. The mass coefficient is changed from zero to 6E-3, while the stiffness coefficient is kept equal to 3E-3. This corresponds to approximately 0.5 % damping at a frequency of 0.5 Hz.
- The upper layer of the soil in the original model is weak. This makes the structure fail below the seabed and causes an increased buckling length. In order increase the load factor and prevent the structure from this failure pattern, different aspects are studied. First, the scaling factor for the force unit used in the soil curves, Ffac, in the function SOILCHAR is increased from 1 to 4. However, this is in practice the same as increasing the diameter four times or using four piles, which is conservative. Bucket foundations at the connection between the piles and the jacket as

additional support is another option studied, see Figure 14. Due to the weak upper layer of the soil, this only gives a minimal increase in the load factor. The conclusion is to increase the pile thickness in PILEGEO from 30 to 50 mm, which results in a more stable structure against sideways failure. In practice, this modification only needs to be done in the upper part of the piles, while the lower thickness can remain small.

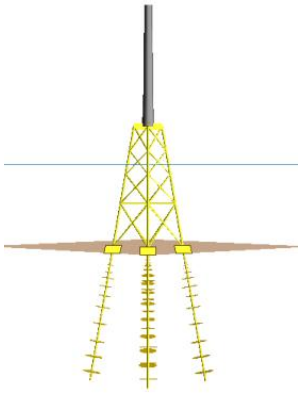

Figure 14: Illustration of bucket foundation

- One desirable failure considering jacket response is the pile on the tension side being pulled out of the soil. This prevents the installation from falling towards the ship. Based on this, the possibility of reducing the length of the piles is studied. However, this result in lack of skin friction along the piles against axial failure and the modification is rejected.

### 3.2.3 Eigenvalue analysis

In order to study the natural periods of the structure, eigenvalue analysis is needed. The natural periods of the wind turbine should be compared to the periods of the environmental loads. The relationship between the natural period, $T$, and the natural frequency, $\omega$, is given as;

$$T = \frac{2\pi}{\omega} \tag{5}$$

It follows from Figure 15, that the dominating load term is the one corresponding to the load frequency (Haver, 2011). In addition, the 2ω and 3ω components are of considerable magnitude. Thereby, correlation between these components and the natural period should be evaluated as it might cause considerable dynamic amplifications, called super-harmonic loading. According to Haver, 90 % out of range from the natural period is acceptable.

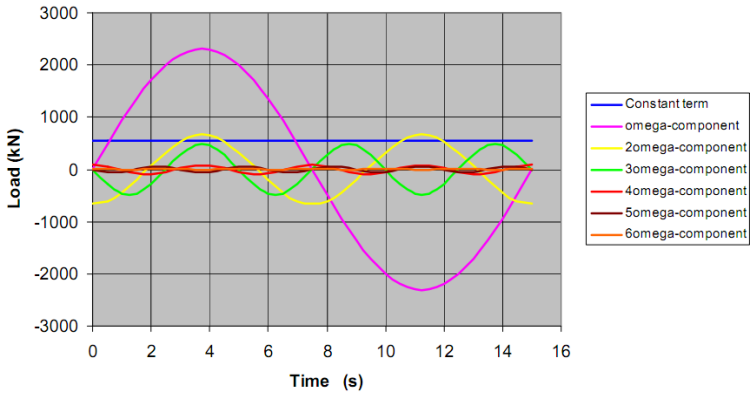


Figure 15: The various Fourier components of total load

The rotor in the wind turbine studied in this work consists of three blades and is performing 5-8 s per rotation (Virtual Prototyping). Based on this, it is desirable to avoid natural periods within the following limit;

$$\frac{[5-8]s}{3blades} \approx [1.7-2.7]s \tag{6}$$

The result from the eigenvalue analysis of the original model is given in Table 5. As seen, the two first natural periods are within the resonance level of the rotor. Figure 16 to Figure 19 displays the mode shapes corresponding to the natural periods.

Table 5: Eigenvalue analysis results

| Mode number | Mode shape | Natural period [s] |
|---|---|---|
| 1 | Cantilever | 2.555540 |
| 2 | Cantilever | 2.555490 |
| 3 | Bending/Sway | 0.852010 |
| 4 | Bending/Sway | 0.851788 |
| 5 | Torsional | 0.696308 |
| 6 | Bending/Buckling | 0.446746 |
| 7 | Bending/Buckling | 0.446715 |

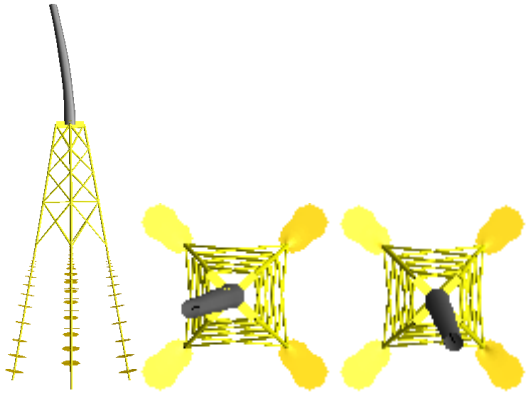

Figure 16: Mode shape 1 and 2

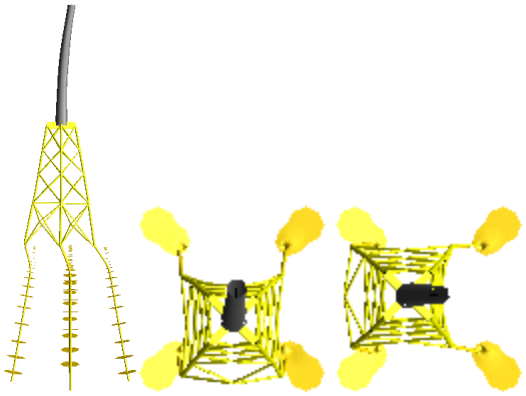

Figure 17: Mode shape 3 and 4

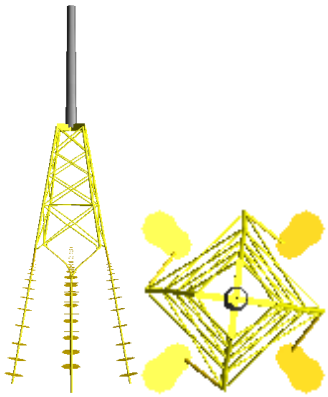

Figure 18: Mode shape 5

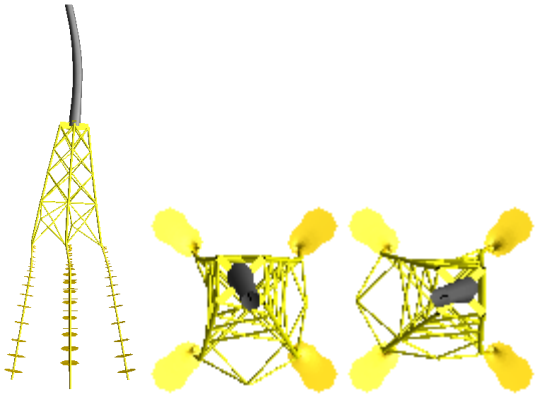

Figure 19: Mode shapes 6 and 7

The resonance problem can be eliminated by increasing the natural period. Based on the equation of motion for a single degree of freedom system and Equation 5, this can be done by reducing the stiffness of the tower;

$$\omega = \sqrt{\frac{k}{m}} \tag{7}$$

$$T = 2\pi\sqrt{\frac{m}{k}} \tag{8}$$

The stiffness, $k$, of a cantilever is given by (Barltrop and Adams, 1991);

$$k = \frac{EA}{l} \tag{9}$$

where $E$ is the elastic modulus, $A$ is the cross-sectional area and $l$ is the length. The stiffness reduction is done by reducing the elastic modulus of the tower from 2.1E5 to 0.84E5 MPa. This results in an increase in the two first natural periods to approximately 3.5 s, and the system is out of the 90 % interval suggested by Haver (Haver, 2011);

$$3.5\ s \cdot 0.9 = 3.1s \neq [1.7 - 2.7]s \tag{10}$$

Table 6 presents the result from the eigenvalue analysis of the modified model used in this research.

Table 6: Modified eigenvalue analysis results

| Mode number | Mode shape | Natural period [s] |
|---|---|---|
| 1 | Cantilever | 3.468520 |
| 2 | Cantilever | 3.468490 |
| 3 | Bending/Sway | 0.803085 |
| 4 | Bending/Sway | 0.802841 |
| 5 | Torsional | 0.615722 |
| 6 | Bending/Buckling | 0.472516 |
| 7 | Bending/Buckling | 0.472463 |

### 3.2.4 Pushover analysis

Static pushover analyses in both storm and operating condition are performed in order to study the reliability of the FE model. The results are presented in the following sections.

#### *Storm condition*

During a storm, the structure is exposed to a Stoke 5$^{th}$ order wave with 20 m height and 12 s period. This represents approximately the 100 year wave in the North Sea. The 100 year wave is a design wave defined as the maximum wave with a return period equal to 100 years.

Due to the increased water depth compared to the original model, sufficient air gap must be checked. A margin of 1.5 m is recommended for fulfilling the ULS criterion (NORSOK, 2007). Without performing a complete air gap analysis and only observing the wave passing the structure, the resulting air gap is found to be approximately 5 m, which is sufficient.

The wave is scaled with an environmental factor of 1.3 and results in a load factor of 1.828, while the original model has a load factor of 2.396. This is within the North Sea requirement of 1.5. Figure 20 show the original model to the left and modified model to the right. Both models experience lateral failure of

the jacket. However, the modified model shows closer interaction between failure in the piles and jacket.

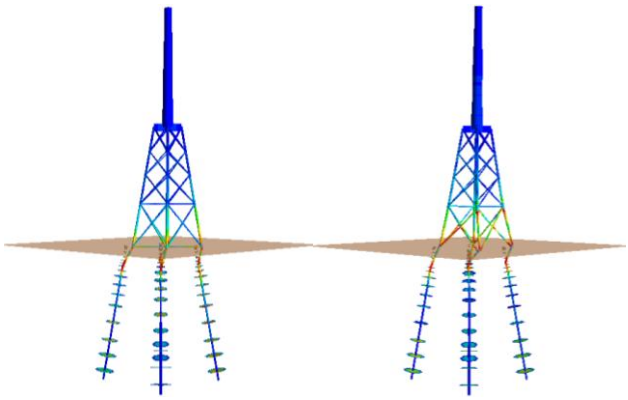

Figure 20: Plastic utilisation of wind turbine exposed to 100 year wave; Left: Original, Right: Modified

### *Operating condition*

During operation the thrust force is included as a 500 kN horizontal point load in top of the tower, acting diagonally on the jacket. The analyses results in a load factor of 11.358 and 10.221 in the original and modified model, respectively. As seen from Figure 21, the tower fails in bending.

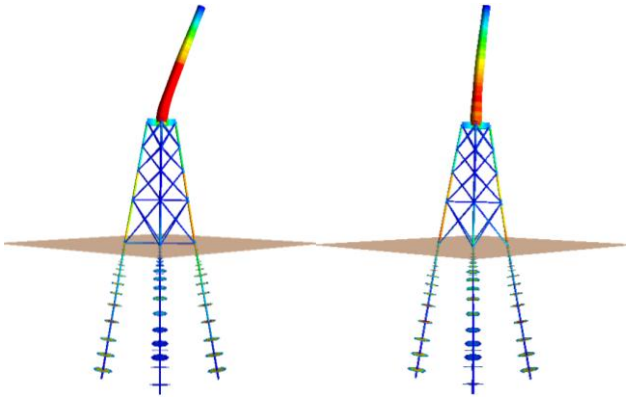

Figure 21: Plastic utilisation of wind turbine exposed to thrust force; Left: Original, Right: Modified

The FE model includes beam theory, which restricts out-of-plane buckling. In order to study potential local buckling of the tower by use of shell theory, hand calculations according to DNVs Recommended Practice c202 "Buckling Strength of Shells" is used (DNV, 2002). Shell elements have curved surfaces. They carry loads by combining membrane forces and bending moments. Shell elements are based on a set of straight beams. The hand calculations are described below. See the Excel file "Shell theory of local buckling of tower" in Appendix B for detailed calculations.

The axial force, $N$, is represented by the turbine weight of 350 kN and bending is caused by the thrust force, $F$, leading to axial and bending stress, respectively;

$$\sigma_x = \frac{N}{2\pi rt} \tag{11}$$

$$\sigma_b = \frac{Fl}{\pi r^2 t} \tag{12}$$

where $r$ is the lower radius of the tower, $t$ is the thickness and $l$ is the length. By use of Table 7 from c202, the Euler and equivalent stress are found;

$$\sigma_E = \frac{C\pi^2 E}{12(1-\nu^2)}(\frac{t}{l})^2 \tag{13}$$

$$\sigma_{eq} = \sigma_x + \sigma_b \tag{14}$$

where $E$ is the modulus of elasticity, $\nu$ is Poisson's ratio and $C$ is the reduced buckling coefficient defined as;

$$C = \Psi\sqrt{1 + (\frac{\rho\xi}{\Psi})^2} \tag{15}$$

Table 7: Buckling coefficients for unstiffened cylindrical shells

| | Ψ | ξ | ρ |
|---|---|---|---|
| Axial Stress | 1 | 0.702Z | $0.5(1+\frac{r}{150t})^{-0.5}$ |
| Bending | 1 | 0.702Z | $0.5(1+\frac{r}{300t})^{-0.5}$ |

ξ and ρ in Table 7 are buckling coefficients, while the curvature parameter Z is defined as;

$$Z = \frac{l^2}{rt}\sqrt{1-\nu^2} \tag{16}$$

The equivalent critical stress is given as;

$$\sigma_{eq,cr} = \frac{\sigma_Y}{\sqrt{1+\lambda_{eq}^4}} = 186\ MPa \tag{17}$$

where $\sigma_Y$ is the yield stress and the equivalent reduced slenderness ratio, $\lambda_{eq}$, is defined as;

$$\lambda_{eq} = \sqrt{\frac{\sigma_Y}{\sigma_{eq}}(\frac{\sigma_x}{\sigma_{x,E}} + \frac{\sigma_b}{\sigma_{b,E}})} \tag{18}$$

As seen from Equation 17, the critical stress is approximately 50 % of the yield stress of 350 MPa. The material factor accounts for deviations from characteristic material and is given by;

$$\begin{matrix} \gamma_m = 1.15 & for\ \lambda_{eq} < 0.5 \\ \gamma_m = 0.85 + 0.60\lambda_{eq} & for\ 0.5 < \lambda_{eq} < 1.0 \\ \gamma_m = 1.45 & for\ \lambda_{eq} > 1.0 \end{matrix} \quad (19)$$

A dynamic amplification factor increasing the nominal thrust force with a factor of 2 is assumed. The environmental factor is set to 1.3, according to ULS design (NORSOK, 2004a). The material factor is found to be 1.45 as Equation 18 that gives $\lambda_{eq}$ larger than one. The design buckling strength is found from;

$$\sigma_{des} = \frac{\sigma_{eq,cr}}{\gamma_m \gamma_e} = 99MPa \quad (20)$$

By setting the utilization equal to one;

$$\eta = \frac{\sigma_{eq}}{\sigma_{des}} = 1 \quad (21)$$

the load factor for the amplified thrust force of 1 000 kN is found to be 1.34, compared to 10.221 when using beam theory. This is outside the safety limit of 1.5 in the North Sea. However, by using a material factor of 1.15, the thrust load factor is increased to 1.7. In addition, the nominal thrust of 500 kN results in a load factor of 2.68. Based on this, the wind turbine is assumed to resist the environmental condition in the North Sea.

## 3.3 Ship impact model

Collision between a large oil tanker and a jacket supported offshore wind turbine involves large kinetic energy. Some of the energy will stay kinetic, while the remaining will dissipate as strain energy in the wind turbine installation due to ductile design discussed in Section 2.3. Collision response of a fixed offshore structure is divided into the following deformation modes corresponding to the NORSOK standard N-004 (NORSOK, 2004b) and illustrated in Figure 22 (Søreide, 1981):

- Local deformation of bracing/leg at the point of impact
- Beam deformation of bracing and leg element
- Overall deformation of platform

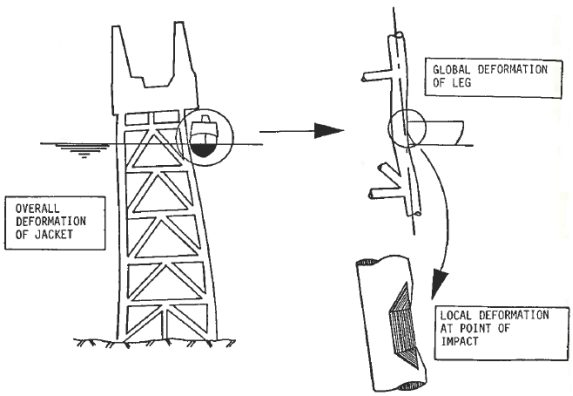


Figure 22: Energy absorption in steel jacket

The BSH standard requires impact analysis for the offshore wind turbine with a ship of 160 000 dwt, corresponding to a displacement of 190 000 tons. This is the size of a Suezmax tanker with approximately 15 m draught and 50 m beam. The wind turbine is assumed to be in operation and wave forces are neglected. The ship is drifting in the wind direction, causing the thrust and impact load acting in the same direction. The direction is set to be 45° counter-clockwise on the positive x-axis, causing corner leg impact.

USFOS provides two impact functions; BIMPACT for static analysis and DYNIMPCT for dynamic analysis. However, an alternative is to model both the offshore wind turbine and the tanker (Holmås, 1999). Contact between the two structures is described as compressing a nonlinear spring with a concentrated load. This indicates conservative results. The springs are defined as hyperelastic, i.e. no elastic unloading and the input curve is followed both in loading and unloading. In reality, some energy is absorbed by the ship. This is neglected in this work, which is conservative regarding the response of the offshore wind turbine. The different impact cases are described in the following sections.

### 3.3.1 Loaded ship joint impact

In order to account for the possibility of a ship with a draught larger than 15 m or shallower water, impact with the joint located at approximately 20 m below the sea surface is studied. Although, this draught might be unrealistic compared to the level normally exposed to ship impact. The joint is a stiff part of the jacket structure. Joint impact will not likely deform the jacket locally, as this requires buckling of all connected bracings before arise of yield hinge and deformation begins, see Figure 23. Based on this, ship-jacket contact is assumed to act in one node only.

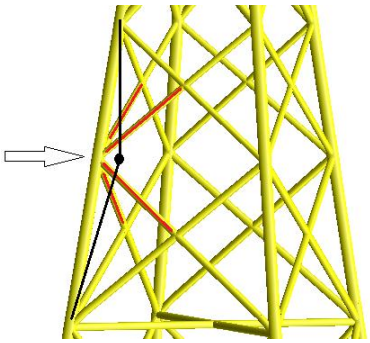

Figure 23: Joint impact with no yield hinge

The simulation is performed by creating a node on a nonlinear spring. The spring is given a compressive stiffness of 500 MN/m. USFOS requires the force-displacement curve to go through the origin, without defining it as a point on the curve. Based on this, the stiffness is defined up to 100 N in tension, which is practically the same as zero in this context. See Figure 24 for spring location and force-displacement curve.

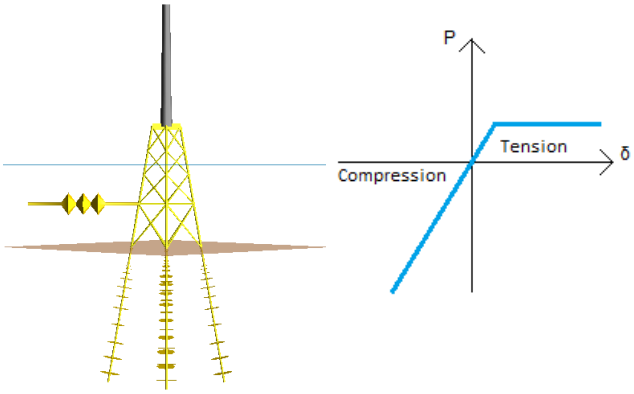


Figure 24: Spring modelling of loaded ship joint impact

### 3.3.2 Ballast ship joint impact

In ballast the ship has a draught of approximately 8 m and impact with the joint at approximately 5 m is studied. The impact energy is smaller in ballast and oil spill is not of concern. Figure 25 shows the modelling of the ballast ship impact. Based on the assumptions regarding joint impact discussed above, the ship is assumed to only hit one node. The spring force-displacement curve corresponds to the curve described for the loaded ship joint impact, given to the right in Figure 24.

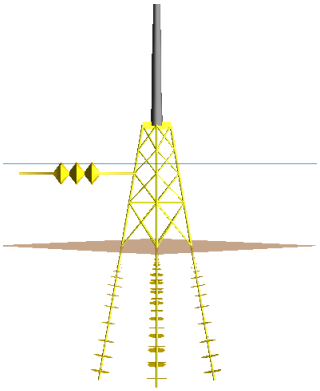

Figure 25: Spring modelling of ballast ship joint impact

### 3.3.3 Loaded ship column impact

The largest width of the hull is assumed located approximately 2 m above the keel. Based on a draught of 15 m, this gives an impact point at 13 m depth. This is located between the two joints defined above. The column is soft, compared to the joint. The inter-joint impact will most likely create a yield hinge. After some deformation of the element, the ship side will reach the joint at 5 m depth, see Figure 26.

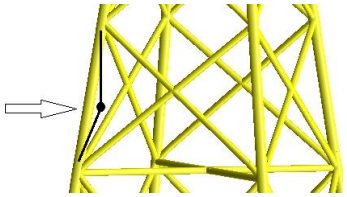

Figure 26: Column impact creating a yield hinge

The midpoint of the element is located at 12.5 m depth, and is chosen to represent the impact location on the column. The element is divided in two and an extra node is included in the model file.

In order to model this impact case, two springs are connected with an infinitely stiff beam, see Figure 27. The loser spring corresponds to the graph to the right in Figure 24. The upper spring experience some compression before it is activated, due to the slope of the jacket leg. This is represented by a lower stiffness, such that the force is practically equal to zero until 1.3 m deformation. This stiffness is defined up to 1.3 m in tension, in order to go through the origin. Beyond this point, the force is 100 N, which is practically equal to zero. See the Excel file “Node interpolation” in Appendix B for calculations of the value 1.3. The force-deformation curve is shown to the right in Figure 27.

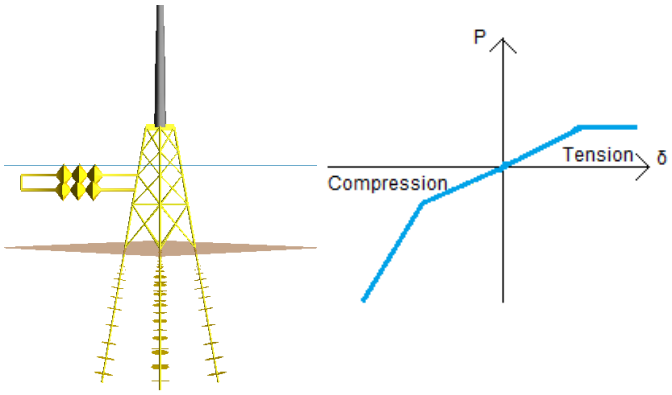


Figure 27: Spring modelling of column impact

# Chapter

# 4. Case Studies

The static and dynamic global analyses of collision between a large oil tanker and an offshore jacket wind turbine are described in this chapter. The nonlinear analyses are executed using USFOS. All quantities in USFOS are expressed in base units.

## 4.1 General

The goal with this research is to verify or invalidate the design requirements in the BSH standard "Design on Offshore Wind Turbines". In order to study whether the installation can be considered "collision friendly", the direction of the failure and the nacelle response is verified. The ship is assumed drifting sideways towards the corner of the wind turbine, impacting one of the jacket legs. The favourable outcome is that the wind turbine collapses in the drift direction of the tanker.

The ship-jacket impact is simulated as a node-to-node spring. In a realistic impact the ship will slide along the jacket leg, changing vertical impact location on the jacket as the installation turn over. In order to reduce the influence of the theoretical formulation, the spring is modelled 1 km long. The ship is assumed to hit the jacket through its centre of gravity without transforming kinetic energy into rotational energy. This is considered the most unfavourable outcome (Søreide, 1981).

## 4.2 Static analysis

Static analysis describes the effect of forces on systems at rest. The effect of immediate change of the system is found, without studying the long term response. Static equilibrium is described as the sum of forces is equal to zero;

$$\sum \boldsymbol{F} = 0 \tag{22}$$

Statically, the installation will transform the collision energy to the soil as shear forces, mainly as axial compression and tension in the bracings (Amdahl and Eberg, 1993).

In the static case the drifting ship is represented by a node given a point load in y-direction. Numerical errors allow the node only to move in one horizontal direction and thereby x-translation is restricted. The ship-jacket contact is simulated as a nonlinear spring, described in Section 3.3. The load is given a random size of 500 kN, increasing towards failure or maximum step. Based on this, no difference is made between loaded and ballast ship impact energy in the static analyses.

## 4.3 Dynamic analysis

A more realistic analysis of the structural behavior during a ship collision is performed dynamically. This includes motion of the system exposed to forces. It describes the time dependent response. The dynamic equation of motion is given as (Søreide et al., 1988);

$$\boldsymbol{F}^i(t) + \boldsymbol{F}^d(t) + \boldsymbol{F}^r(t) - \boldsymbol{R}(t) \tag{23}$$

where $\boldsymbol{F}^i$, $\boldsymbol{F}^d$ and $\boldsymbol{F}^r$ is the inertia, damping and restoring forces, respectively, and $\boldsymbol{R}$ is the external loads.

The node representing the ship is given a mass with initial velocity, corresponding to the impact speed of 2 m/s. The mass in loaded condition is set to 266 000 tons according to the BSH requirements including 40 % added mass for sideways ship collision. In ballast the mass is set to 70 000 tons, corresponding to a total mass of 98 000 tons including added mass. It follows from Equation 2 that the two conditions involves energy equal to;

$$E_{loaded} = 532\ MJ \tag{24}$$

$$E_{ballast} = 196\ MJ \tag{25}$$

In the dynamic analyses, both horizontal directions is allowed to be free. However, this requires that the functional loads, including the thrust force, are applied dynamically due to the static restriction. Thereby, the axial forces in the elements are not fully developed before the impact begins. The functional loads are applied during the first second, while the impact begins after two seconds. The effect of applying the functional loads dynamically is observed to have small effect on the results, see the axial stress in the installation and the force in top of the tower in Figure 28.

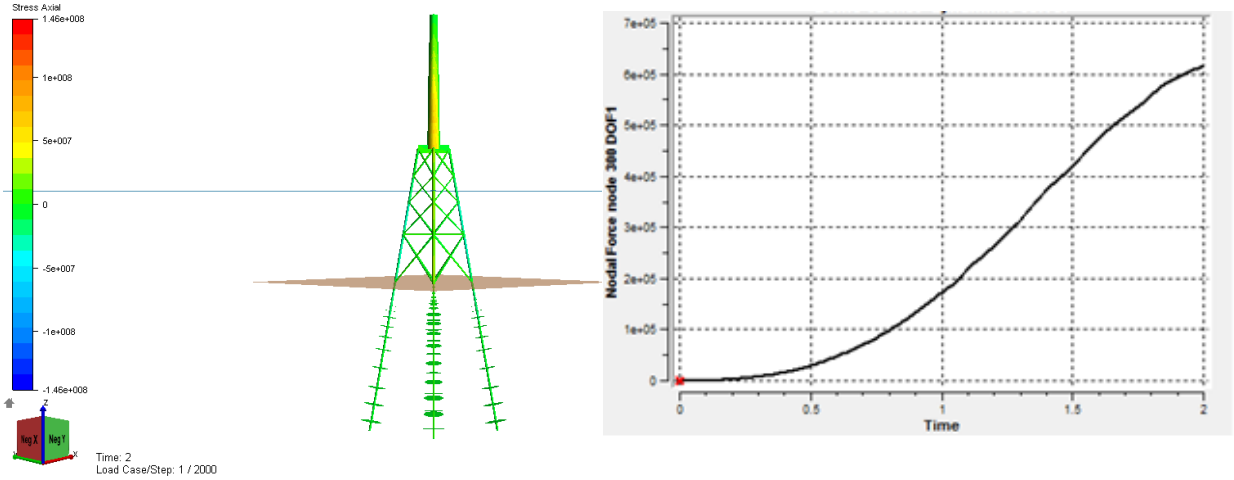


Figure 28: Axial stress at 2 s and force in top of tower when applying functional loads dynamically

Large inertia forces due to the weight of the turbine might cause compression on the impact side. The tower is studied elastically in order to account for local buckling. Axial stress is scaled according to the design stress described in Section 3.2.4. Ship impact is designed according to accidental limit state (ALS), where the action factors are equal to 1.0 (NORSOK, 2004a). According to Equation 17 this gives a design buckling strength equal to;

$$\sigma_{des} = \sigma_{eq,cr} = 186\ MPa \tag{26}$$

In addition the shape factor for pipe cross-sections, $\alpha$, should be included (Amdahl, 2005);

$$\alpha = \frac{W_p}{W_e} = \frac{M_p}{M_e} = \frac{4}{\pi} \tag{27}$$

where $W_p$ and $W_e$ is the plastic and elastic section modulus, respectively, and $M_p$ and $M_e$ is the plastic and elastic bending moment, respectively. The shape factor represents reserve capacity, which describes the structures ability of carrying bending moment after first yield. This results in an elastic design buckling strength defining the buckling strength of the tower accounting for local buckling of;

$$\sigma_{des,e} = 186 \cdot \frac{\pi}{4} = 146\ MPa \tag{28}$$

Exceeding the design limit might involve the tower falling towards the ship.

The steel jacket has reserve strength beyond first yield and is studied plastically. The NORSOK standard N-004 “Design of steel structures” suggests a critical average strain in axially loaded elements according to;

$$\varepsilon_{cr} = 0.02 + 0.65\frac{t}{l} \tag{29}$$

where $t$ is the plate thickness and $l$ is the length of the plastic zone (minimum $5t$) (NORSOK, 2004b). The critical strain is set to 15 %, according to S 355 steel. Fracture in tension bracings is checked according to this value.

Failure of the nacelle fixation is studied by comparing the acceleration in top of the tower to the nacelle bolt acceleration limit of 1 G.

# Chapter

# 5. Results

This chapter presents the results from the static and dynamic analyses of the ship-wind turbine impact. The BSH wind turbine requirement of no major environmental pollution due to the collision is studied. The results are based on a FEA including beam theory. Forces in the contact spring and plastic utilization of the installation are enclosed in Appendix A. In addition, it includes the time variation of the ship velocity and velocity in the impact node from the dynamic analyses.

The ship impact is acting 45° counter-clockwise on the positive x-axis. Based on this, the quantities in the impact direction are calculated by use of Pythagorean Theorem;

$$a^2 = b^2 + c^2 \tag{30}$$

In case of symmetrical failure, only x-directional results are presented. The failure pattern- and plastic strain screenshots are originated with the ship entering from the left, while the axial stress figures are viewed from the direction of the impact.

## 5.1 Static analysis

As described in Section 4.2, static analysis describes the immediate effect of forces on systems at rest and is not time dependent. Thereby, inertia causing compression and local buckling on the hit side of the tower is not of concern. The static failure patterns are displayed after 200, 300, 400 and last step.

### 5.1.1 Loaded ship joint impact

Static analysis of the collision between the loaded ship and wind turbine in the joint located 20 m below the sea surface is executed. It results in lateral displacement with failure in the piles below the seabed due to the weak upper layer in the soil, displayed in Figure 29. The failure is unsymmetrical and the horizontal displacement in top of the tower is given in Figure 30. The installation mainly translates in the positive x-direction. Based on this, the tower collapses away from the ship and will not destruct the ship deck causing environmental pollution. The asymmetric failure appears after the slope change in the global energy curve given in Figure 31, between step 300 and 400. This is caused by failure in the pile in the front of the jacket in Figure 29.

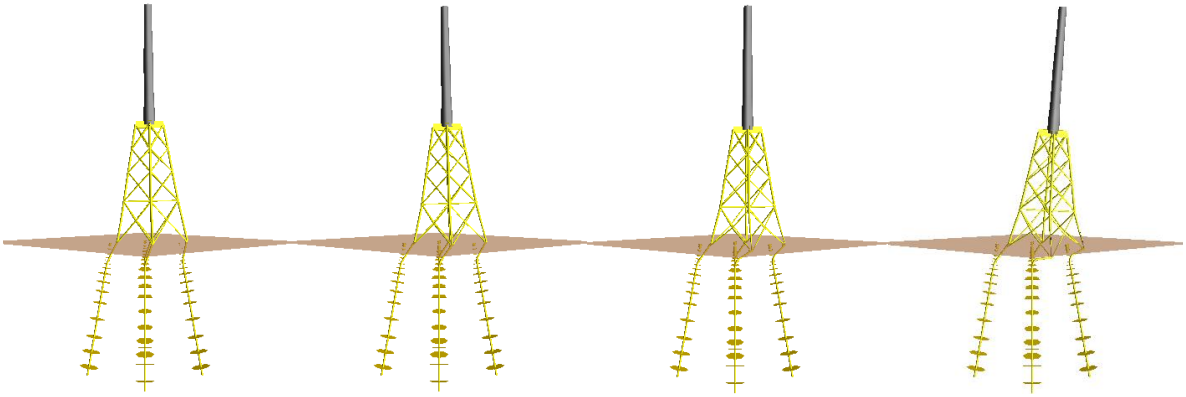

Figure 29: Static failure pattern for loaded ship joint impact

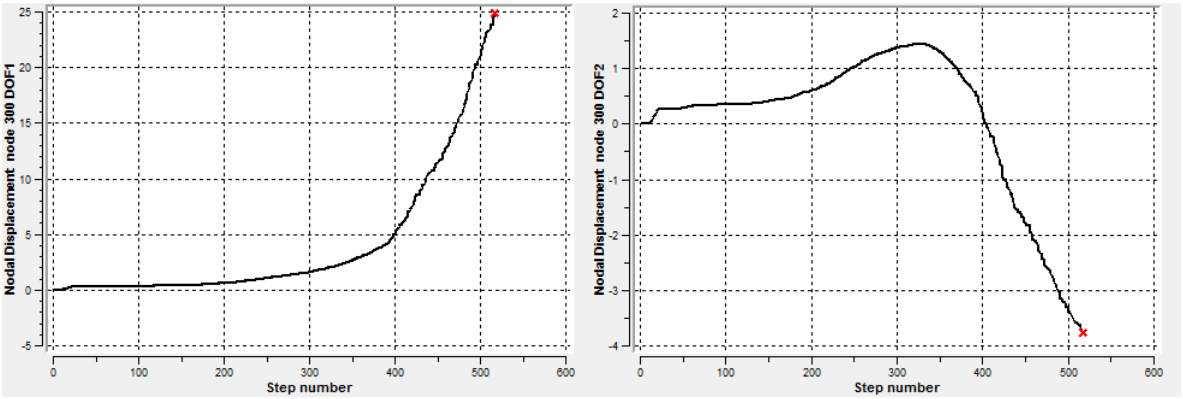


Figure 30: Static displacement in top of tower for loaded ship joint impact

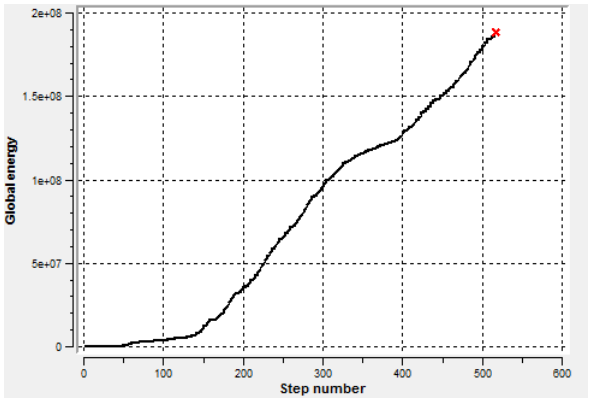


Figure 31: Static global energy for loaded ship joint impact

### 5.1.2 Ballast ship joint impact

The failure of the wind turbine due to impact with the joint at 5 m depth with a ship in ballast is shown in Figure 32. Contrary to the loaded ship, the failure is axial and symmetric. Axial failure involves the pile on the tension side being pulled out of the soil. Also this case induces failure in the foundation. The displacement in x-direction in top of the tower is given in Figure 33. The impact results in outwards buckling of the opposite sided leg. This marks the slope change in the energy curve, seen at step 175 in Figure 34. The ship forces the wind turbine to collapse away from the ship. As seen from Figure 34, less

energy is absorbed compared to the loaded ship, although the impact force is equal. This is due to the buckling of the leg, decreasing the energy dissipation ability.

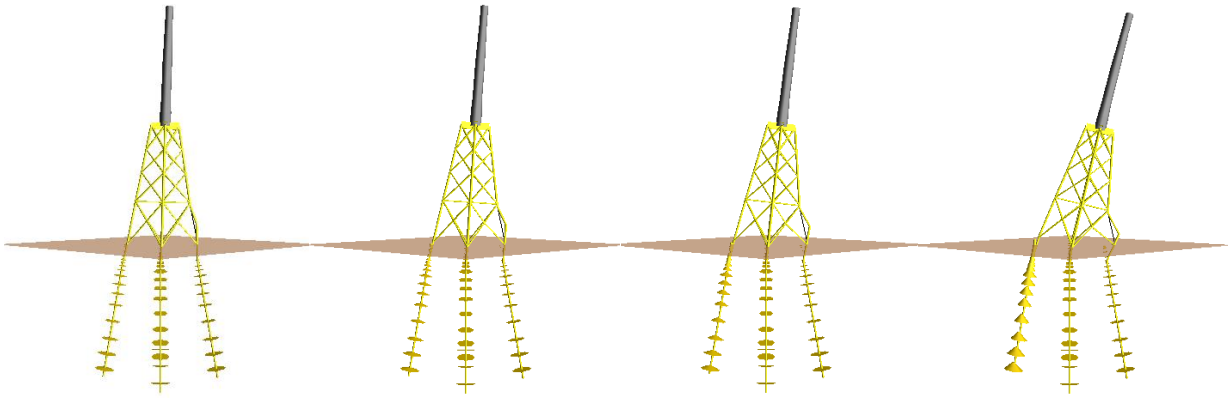

Figure 32: Static failure pattern for ballast ship joint impact

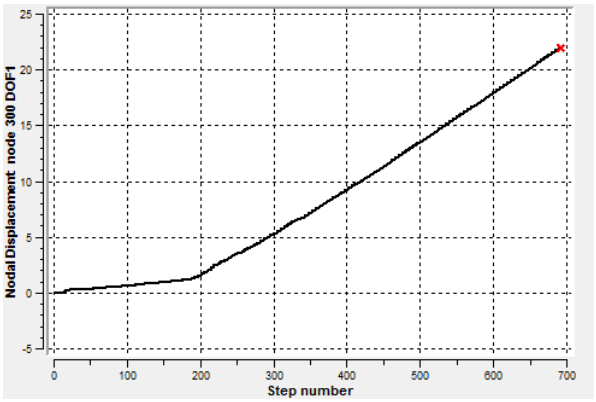


Figure 33: Static displacement in top of tower for ballast ship joint impact

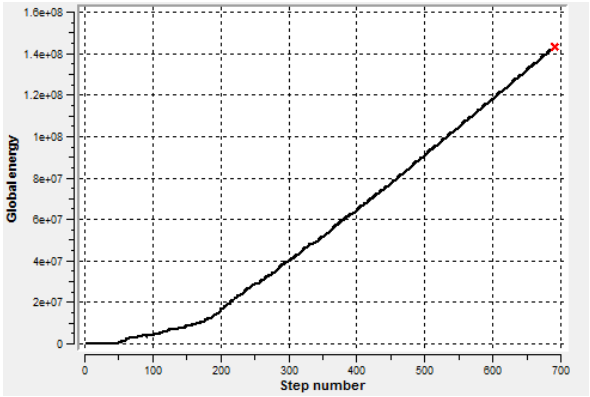


Figure 34: Static global energy for ballast ship joint impact

### 5.1.3 Loaded ship column impact

The ship-jacket impact at 12.5 m results in local deformation of the jacket leg, seen after 200 steps to the left in Figure 35. A second impact location is created due to deformation of the column, as described in Section 3.3.3. Beyond this, global deformation of the installation is activated. At the beginning of the analysis, axial failure pulls out the pile on the impact side. After this, outwards buckling of the opposite leg occurs with failure below the seabed. The wind turbine is collapsing symmetrical in the horizontal

direction, away from the ship. The x-directional displacement in top of the tower is given in Figure 36. The global energy is given in Figure 37. The column impact is comparable to the ballast ship joint impact described above. The two impact models share one impact point giving the same overturning height.

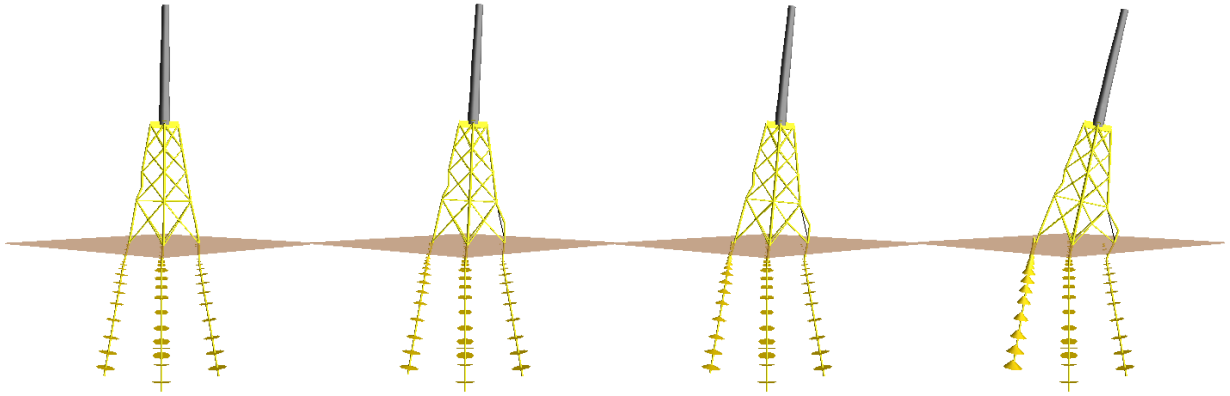

Figure 35: Static failure pattern for loaded ship column impact

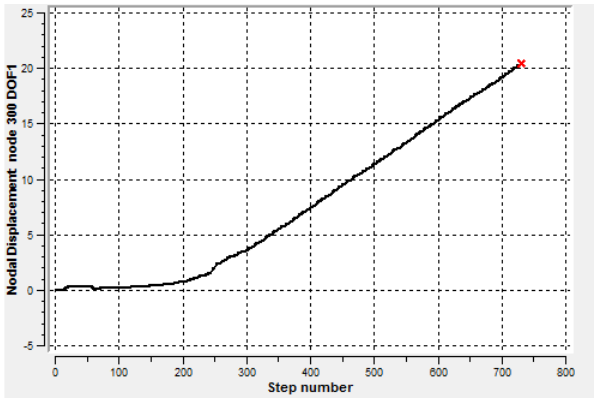


Figure 36: Static displacement in top of tower for loaded ship column impact

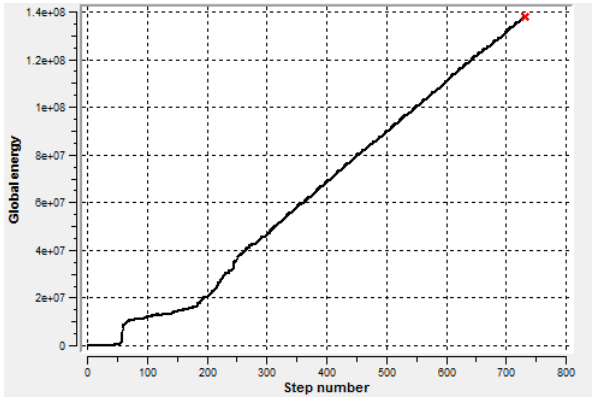


Figure 37: Static global energy for loaded ship column impact

## 5.2 Dynamic analysis

The length of the dynamic simulations is decided from the failure development. The analysis is stopped before collapse, in order to avoid the large values in the graphs from the final collapse, such that the early stage results are better displayed.

The dynamic failure patterns are displayed after 4, 6, 8 and 10 s. Local buckling of the tower is studied dynamically by scaling the axial stress according to the calculated design value of 146 MPa. The axial stress screenshots are taken at maximum compression on the impact side of the tower in order to verify the possibility of collapse towards the ship. Fracture is studied dynamically by scaling the plastic strain to 0.15, suggested by NORSOK. The plastic strain figures are from 8 s of simulation. Accelerations are evaluated according to the nacelle bolts fixation criterion of 1 G.

### 5.2.1 Loaded ship joint impact

The loaded ship impact in the joint at 20 m depth is comparable to the static analysis with lateral failure of the jacket, see Figure 38. The piles and soil fail, while the jacket remains intact. However, the dynamic results give a symmetrical collapse. The x-directional displacement graph of the top node in the tower is given in Figure 39. As seen, the installation is not able to withstand the ship force and results in the installation falling away from the ship. The global energy in the wind turbine is displayed in Figure 40.

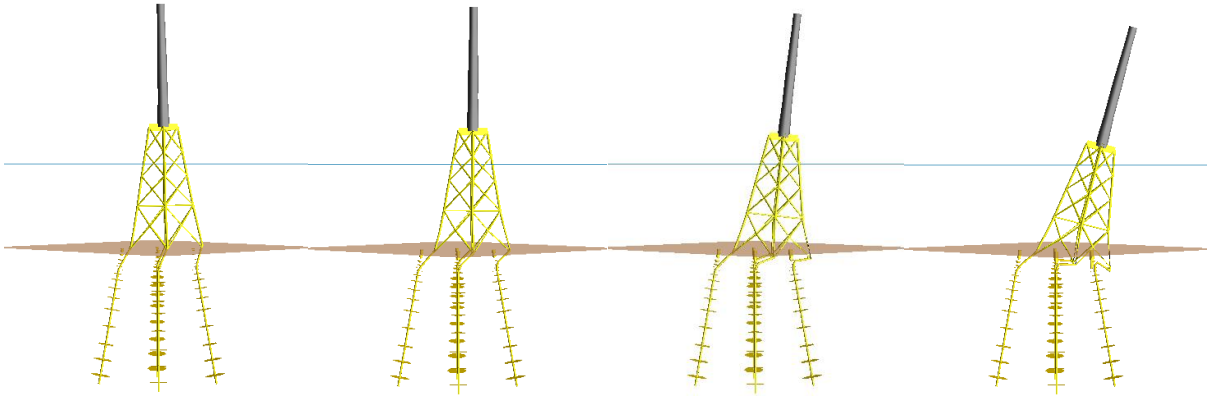

Figure 38: Dynamic failure pattern for loaded ship joint impact

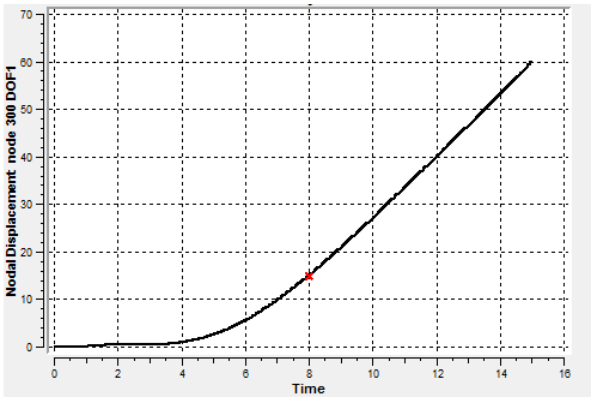


Figure 39: Dynamic displacement in top of tower for loaded ship joint impact

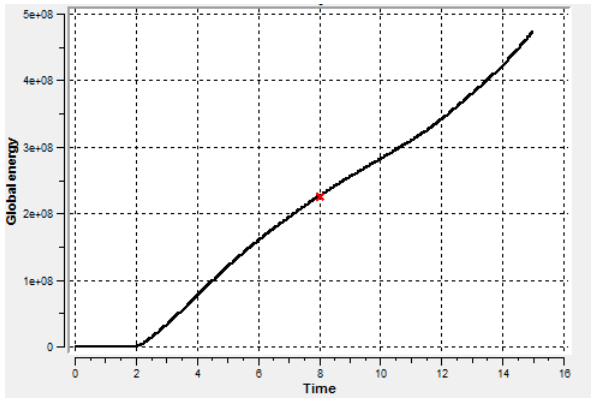


Figure 40: Dynamic global energy for loaded ship joint impact

As seen to the left in Figure 41, the stress limit of 146 MPa is not exceeded in the tower. Based on this, no local buckling is present on the impact side of the tower in this case and failure towards the ship is not of concern. To the right in Figure 41, the plastic strain is illustrated. The lower tension bracing on the impact leg is close to exceeding the limit of 0.15. However, this is beyond 10 s of simulation and the collapse is well developed, such that fracture is assumed not to affect the collapse pattern significantly.

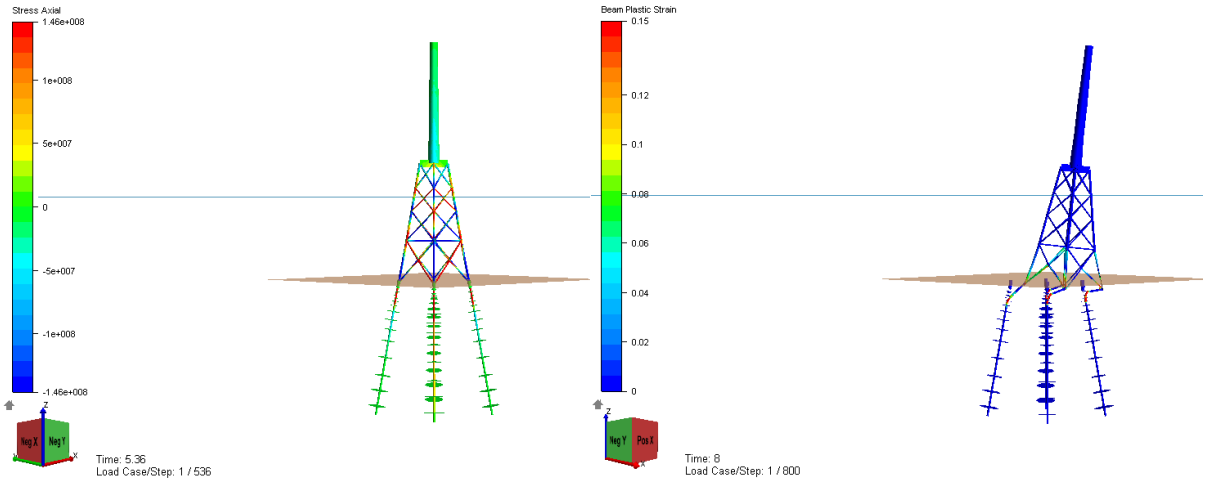


Figure 41: Dynamic axial stress and plastic strain for loaded ship joint impact

Figure 42 displays the x-directional velocity and acceleration in top of the tower during the ship impact. The velocity is increasing rapidly at the beginning of the impact as the tower is forced laterally. When overturning of the wind turbine dominates the failure pattern, the horizontal velocity is stabilizing. As seen to the right in Figure 42, there is a peak in the acceleration at the beginning of the impact when the ship hits the jacket of approximately 3 m/s$^2$. The nacelle fixation criterion of 1 G is not exceeded. Based on this, the nacelle is not expected to drop down on the ship and penetrate the deck.

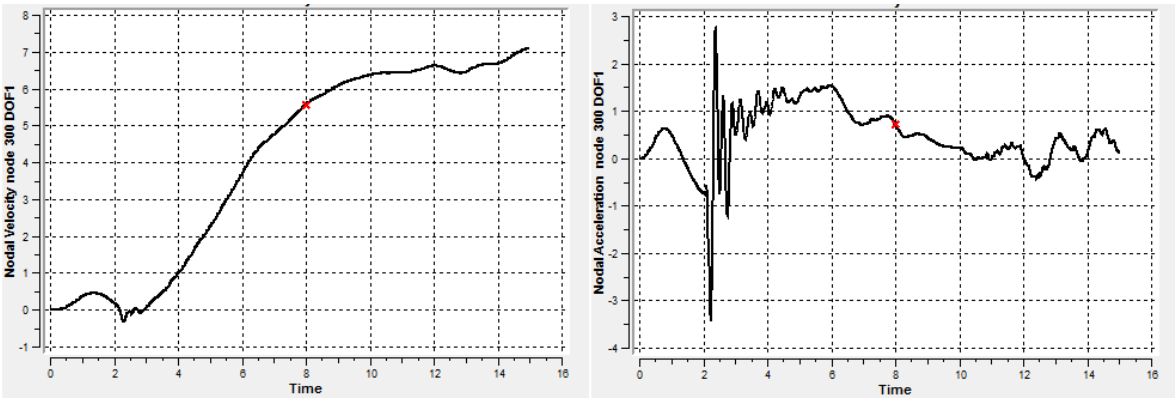


Figure 42: Dynamic velocity and acceleration in top of tower for loaded ship joint impact

### 5.2.2 Ballast ship joint impact

The failure pattern and nacelle displacement due to impact with the upper joint in ballast is shown in Figure 43 and Figure 44, respectively. The ship force causes symmetrical sideways displacement of the jacket at the beginning of the analysis. This is followed by axial failure of the jacket and failure of the soil. The pile on the tension and compression side is pulled out and pushed into the soil, respectively. Finally, the opposite leg buckles inward, contrary to the static analysis that buckles outwards. The installation fails away from the ship and destruction of the ship hull due to global deformation of the jacket is not expected. The wind turbine dissipates the collision energy and stops the ship. The impact results in a global energy of approximately 300 MJ, given in Figure 45.

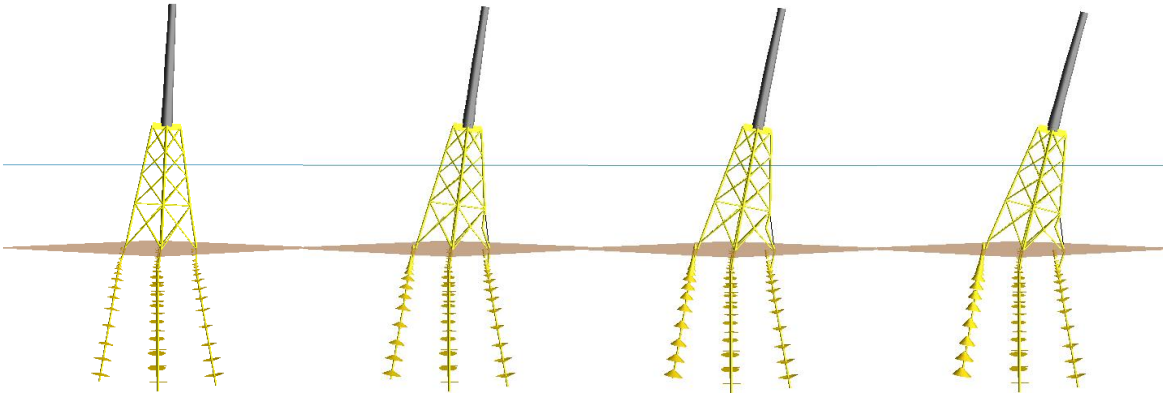

Figure 43: Dynamic failure pattern for ballast ship joint impact

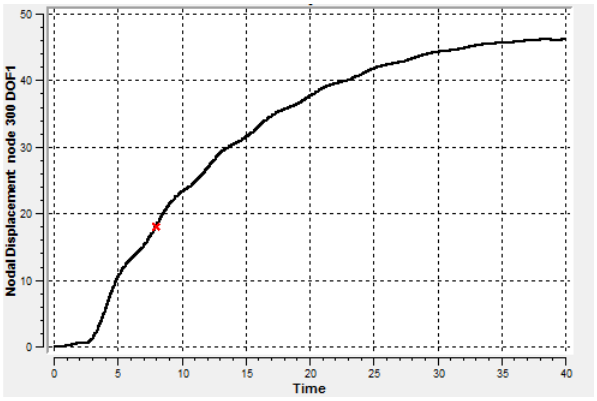


Figure 44: Dynamic displacement in top of tower for ballast ship joint impact

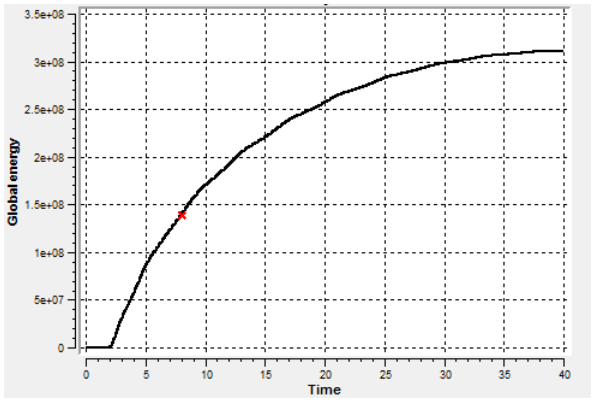


Figure 45: Dynamic global energy for ballast ship joint impact

The highest compressive stress on the impact side of the wind turbine tower during the analysis is given to the left in Figure 46. The stress is exceeding the elastic limit of 146 MPa at the beginning of the analysis when the ship hits the jacket. This implies that local buckling might occur and can cause tower failure towards the ship. Beyond this point, compressive forces are only acting on the opposite side of the tower. To the right in Figure 46, the plastic strain is displayed. The limit of 15 % elongation of the tension bracings is not exceeded.

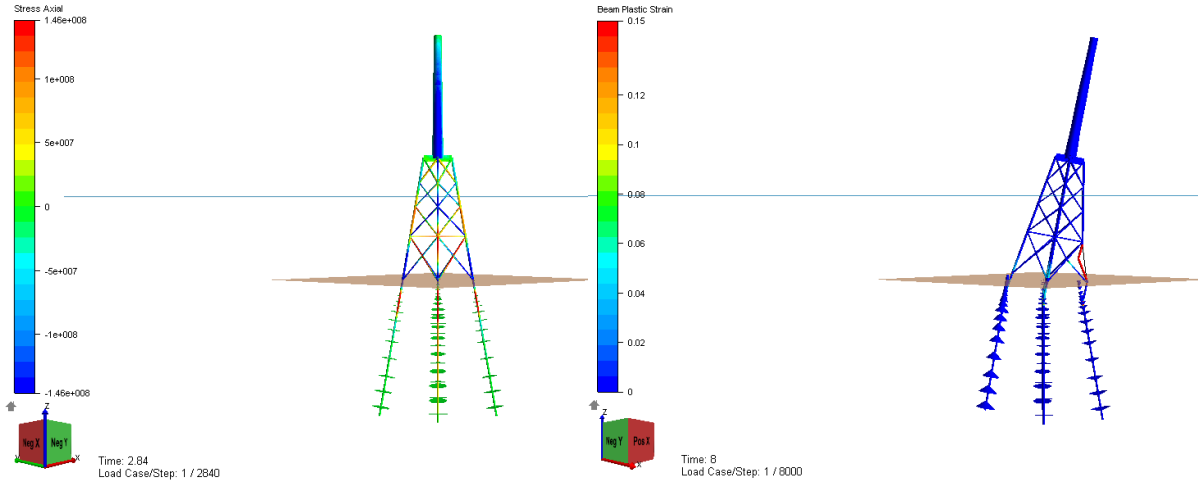


Figure 46: Dynamic axial stress and plastic strain for ballast ship joint impact

Figure 47 gives the time variation of the horizontal velocity and acceleration in top of the tower. Comparing the graphs to the results from the impact with a loaded ship, the dynamics in the tower is increased. After the impact energy is dissipated, response similar to simple harmonic motion is observed in the tower (Barltrop and Adams, 1991). The mass in top of the tower accelerate and oscillate the system. However, damping of the system diminishes the oscillation. The peak in the acceleration in top of the tower when the ballasted ship hits the wind turbine is causing the large compressive stress described above. The acceleration plots shows that the nacelle fixation criterion of 1 G is not exceeded and the bolts are assumed to remain intact. As seen, the maximum acceleration is higher than for the loaded ship impact and is approximately 5 m/s$^2$. This is caused by the location of the impact. The difference between the joints is 15 m. In this case, the impact is located higher and thereby causing larger overturning moment.

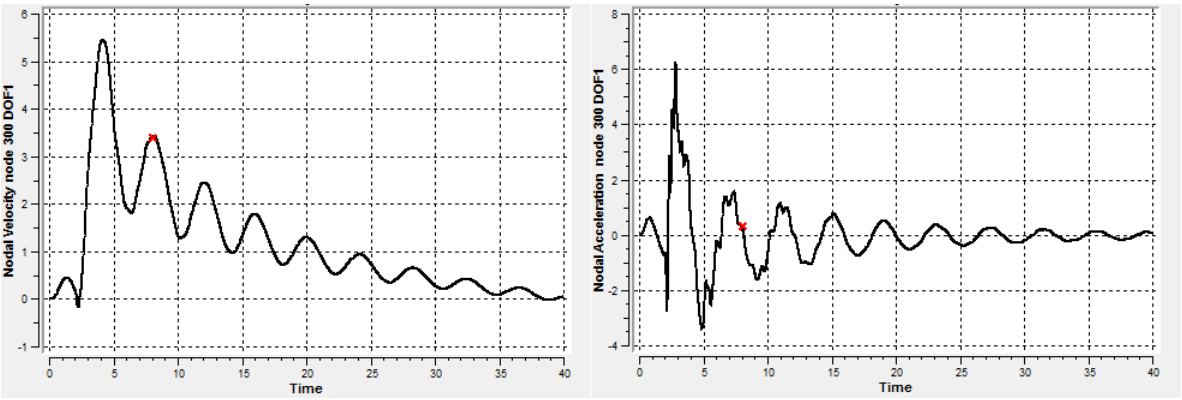


Figure 47: Dynamic velocity and acceleration in top of tower for ballast ship joint impact

### 5.2.3 Loaded ship column impact

Comparable with the static analysis of the inter-joint ship collision, the dynamic impact involves axial failure of the jacket, see Figure 48. The column impact deforms the element, causing a second impact location in the joint at 5 m depth. The impact begins with lateral displacement of the jacket, followed by outwards buckling of the opposite leg with failure below the seabed. The impact leg is pulled out of the soil due to lack of skin friction. The failure is symmetrical and the horizontal displacement in top of the tower is given in Figure 49. The global energy is shown in Figure 50. The wind turbine is not capable of dissipating all impact energy, and is pushed away from the ship.

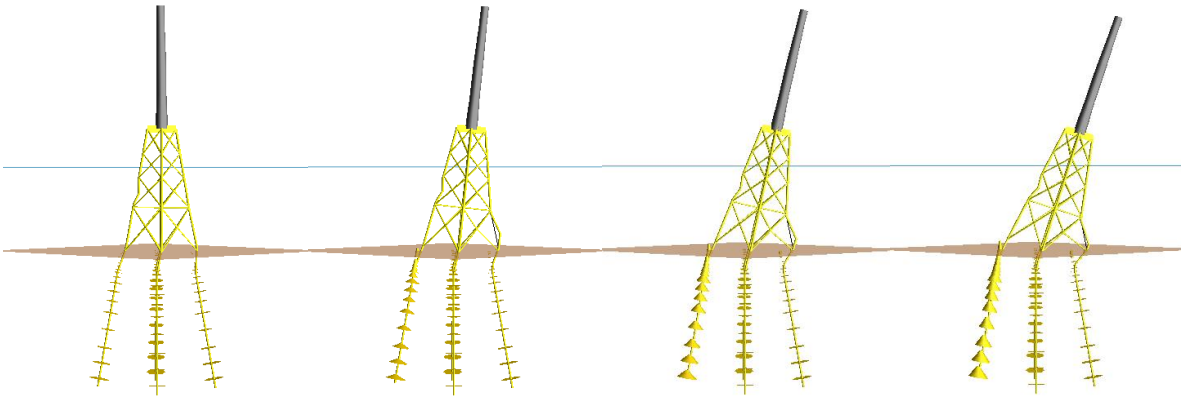

Figure 48: Dynamic failure pattern for loaded ship column impact

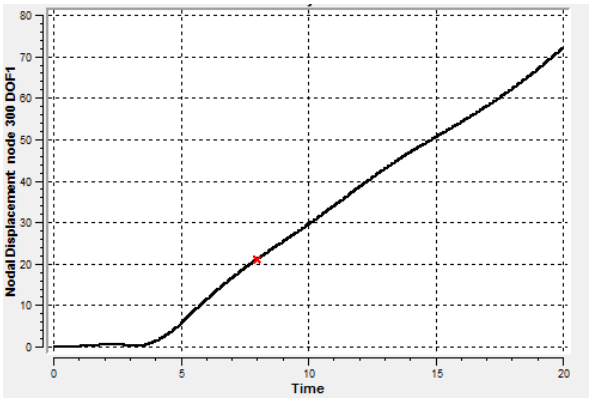


Figure 49: Dynamic displacement in top of tower for loaded ship column impact

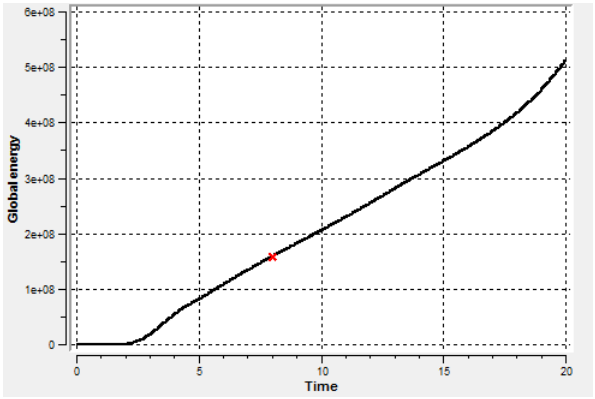


Figure 50: Dynamic global energy for loaded ship column impact

Large compressive forces on the impact side of the tower are observed at an early stage of the simulation, see the left model in Figure 51. This might introduce local buckling in the wind turbine tower and collapse towards the ship. Beyond this, the compression is developing on the opposite of the tower. From the plastic strain screenshot to the right in Figure 51, the values are observed to be below the S355 limit of 0.15 in all tension bracings during the analysis.

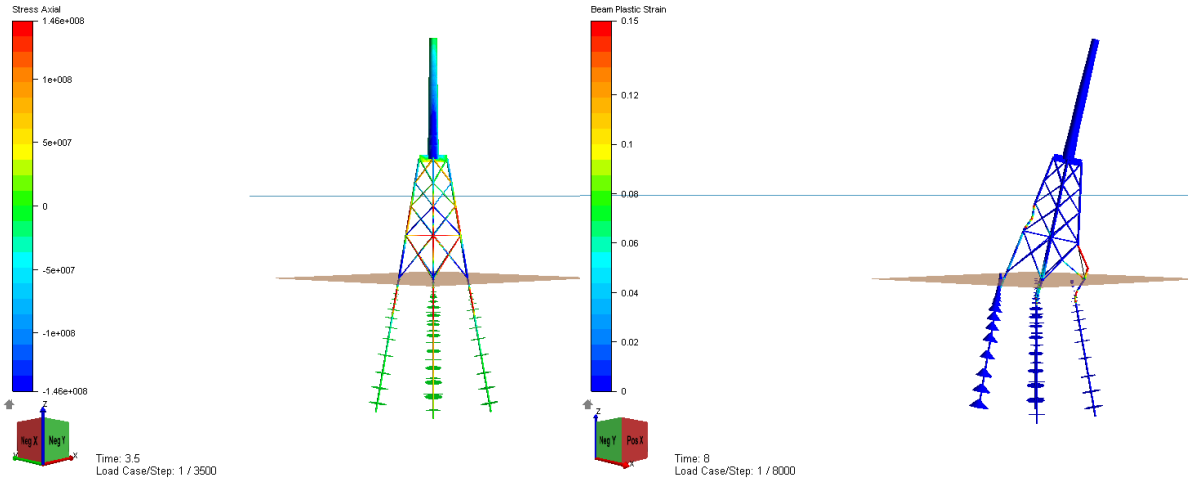


Figure 51: Dynamic axial stress and plastic strain for loaded ship column impact

Figure 52 gives the horizontal velocity and acceleration in top of the tower. The buckling strength described above appears during the peak in the acceleration. As seen, the fixation criterion of the nacelle is not exceeded and the nacelle is prevented from dropping on the ship deck. The maximum acceleration is larger than the loaded ship impact at the 20 m depth, due to the larger height as discussed in Section 5.2.2.

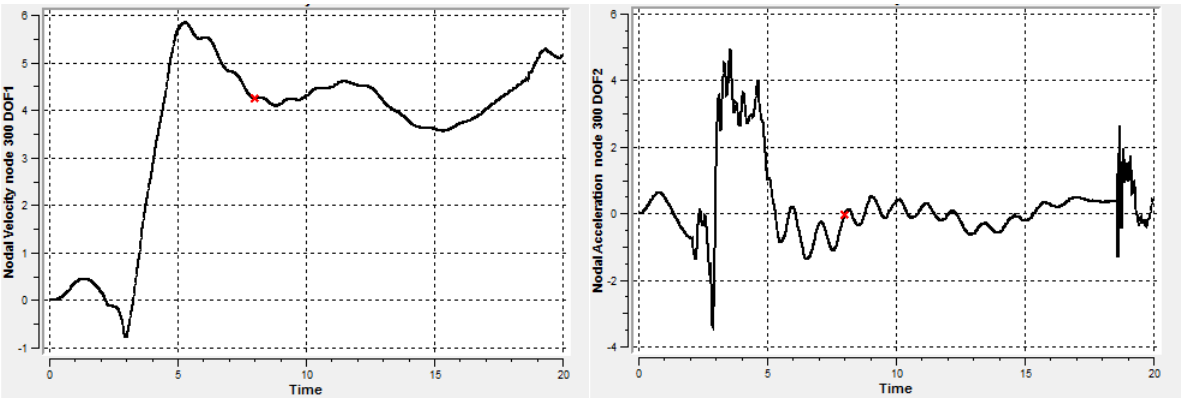


Figure 52: Dynamic velocity and acceleration in top of tower for loaded ship column impact

# Chapter

# 6. Sensitivity Studies

The theoretical description of the true collision scenario might give unreliable results. In order to evaluate the quality of the analyses in this research and discuss the obtained results, sensitivity studies are conducted. Different parameters assumed to affect the analyses are varied and the results are compared to the case studies results presented in Chapter 5. Sensitivity studies are only performed dynamically. The chapter mainly focuses on the loaded ship impact, as this is of interest considering environmental pollution and evaluating the possibility of achieving the BSH wind turbine design check.

## 6.1 Offshore wind turbine modelling

This section studies the modelling of the offshore wind turbine. The soil characteristics are verified, the effect of including imperfections in the installation is evaluated and influence of modifying the tower stiffness in order to avoid resonance is examined. In addition, a more accurate model considering local buckling is analysed by including shell elements in the tower.

### 6.1.1 Soil condition

The model is observed to fail below the seabed in the results presented in Chapter 5. This is due to the weak upper layer of the soil discussed in Section 3.2.2. This causes a soft response of the jacket. The soil parameters are received from Virtual Prototyping and are based on logical reasoning as well as available geological values from the North Sea. The increased pile thickness during the model modifications did not completely prevent buckling below the seabed, but only postponed it. The influence of the soil on the failure pattern is studied by fixing the jacket to the seabed. Numerically this is done by removing the soil file from the analyses. This activates the boundary code “1 1 1 0 0 0” in the four lowest nodes placed at the seabed, discussed in Section 3.2.1. The failure patterns are displayed after 4, 6, 8 and 10 s, with the ship drifting from the left.

#### *Loaded ship joint impact*

The collapse of the offshore wind turbine due to a loaded ship joint impact when the jacket is fixed to the seabed is given in Figure 53. As seen, the pattern is different compared to the analyses including soil. Failure in the soil is replaced with collapse of the jacket. The plots of the x- and y-displacement in top of the tower, given in Figure 55, show an unsymmetrical failure of the wind turbine. This is caused by buckling of the leg in the back in Figure 53. In addition to some negative y-translation, the tower mainly falls in the negative x-direction. Negative horizontal translation indicates motion towards the ship. Failure directly towards the ship deck will likely cause the nacelle falling into the sea behind the ship, due to the large height of the wind turbine. However, in this case the tower does not fall directly over the ship deck and there is a possibility of the nacelle actually hitting the fore or aft part of the ship. The failure is seen from above in Figure 54. Based on this, impact at 20 m depth in solid soil might be critical. The energy absorbed by the installation is shown in Figure 56.

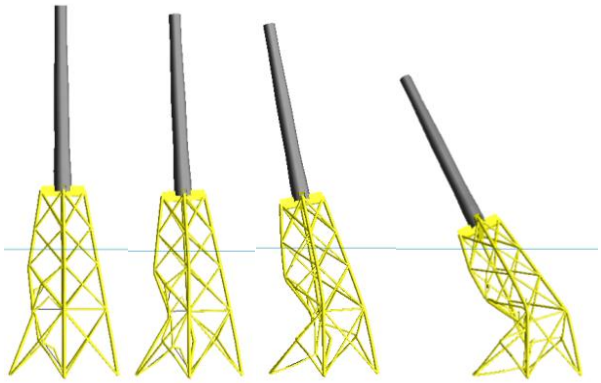

Figure 53: Failure pattern for loaded ship joint impact fixed at seabed

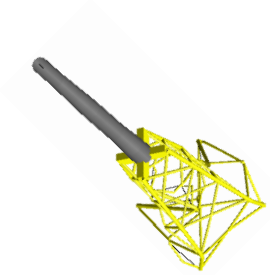

Figure 54: Failure pattern for loaded ship joint impact fixed at seabed seen from above

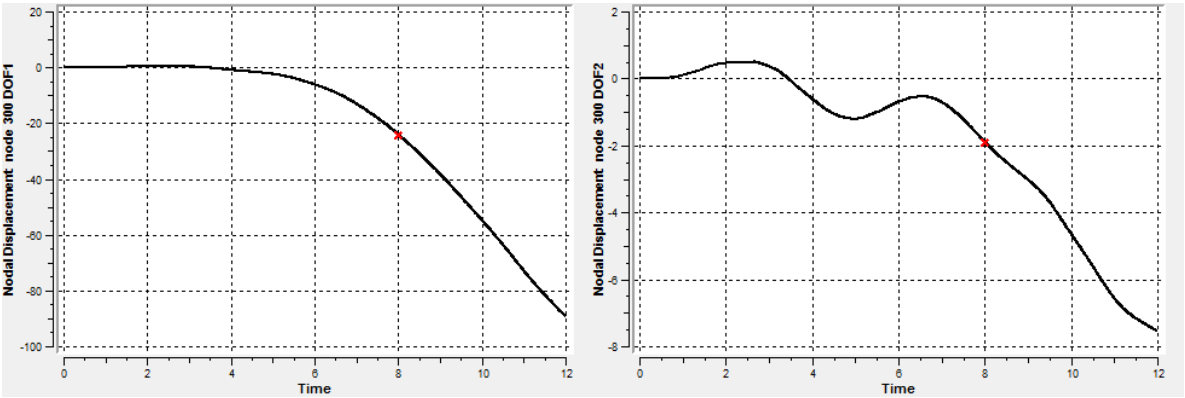


Figure 55: Displacement in top of tower for loaded ship joint impact fixed at seabed

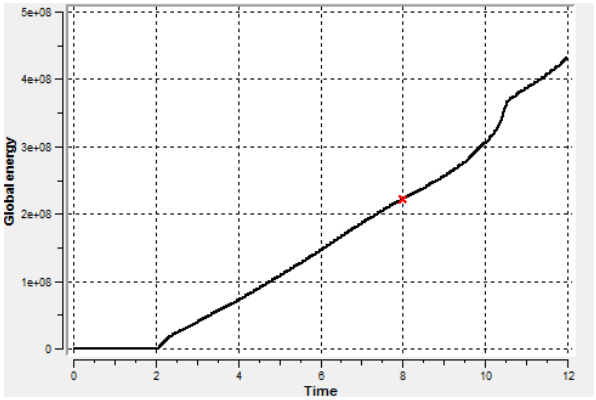


Figure 56: Global energy for loaded ship joint impact fixed at seabed

Figure 57 gives the horizontal velocity and acceleration in top of the tower with the x-directional results at the top and y-directional below. As seen and described from the displacement graphs, the tower mainly moves in the negative x-direction. The nacelle will not disengage from the tower due to acceleration, based on the fixation criterion of 1 G. However, some increase is observed in the acceleration, compared to the results including the soil.

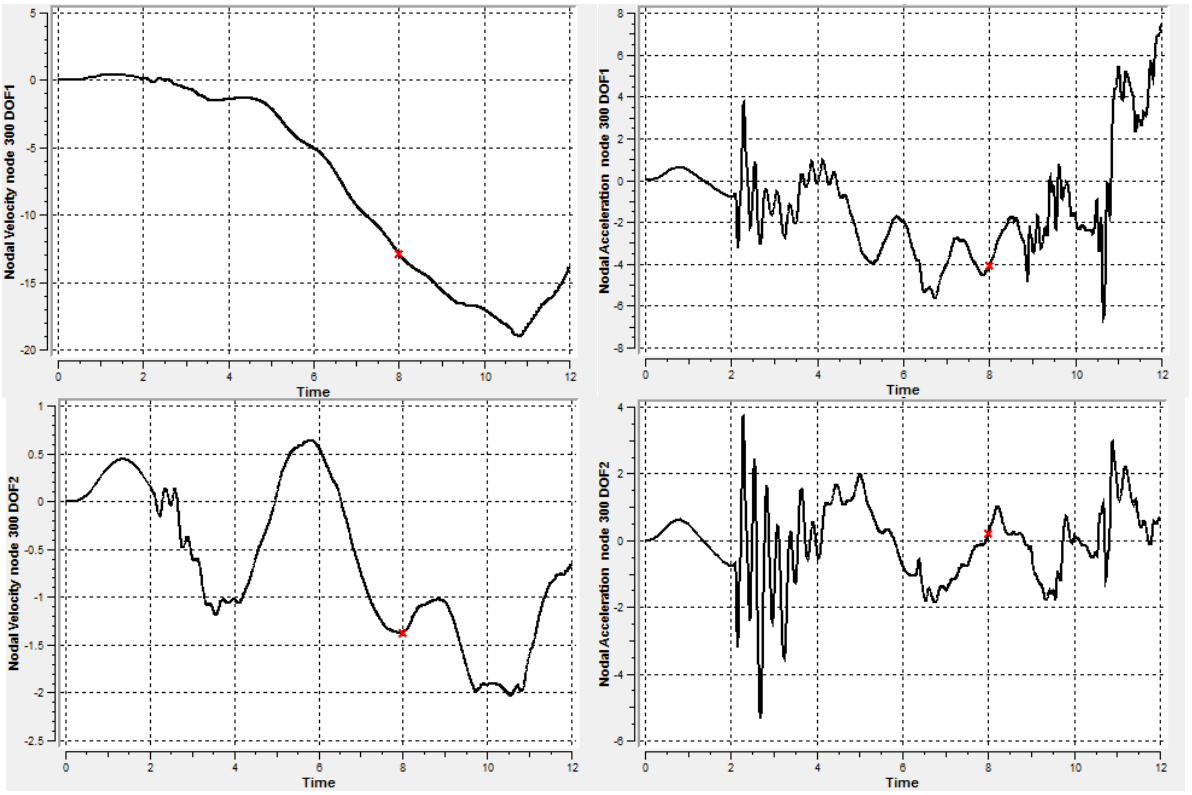


Figure 57: Velocity and acceleration in top of tower for loaded ship joint impact fixed at seabed

## *Ballast ship joint impact*

Failure due to a ship in ballast hitting the fixed wind turbine in the joint 5 m below the sea surface is given in Figure 58. The wind turbine withstands the ship collision with large deformation of the jacket structure. The translation of the installation is symmetric and the x-directional displacement in top of

the tower is given in Figure 59. As seen, equilibrium is reached with the tower oscillating around 2.25 m in the negative x- and y-direction. The global energy is given in Figure 60. As seen, the equilibrium is reached at an earlier stage compared to the original case study.

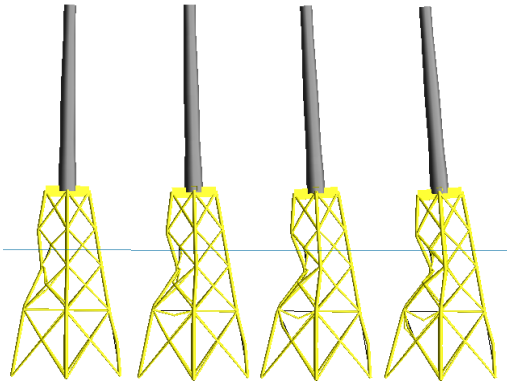

Figure 58: Failure pattern for ballast ship joint impact fixed at seabed

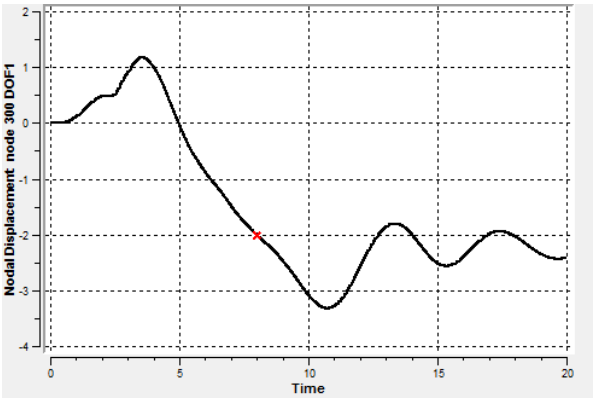


Figure 59: Displacement in top of tower for ballast ship joint impact fixed at seabed

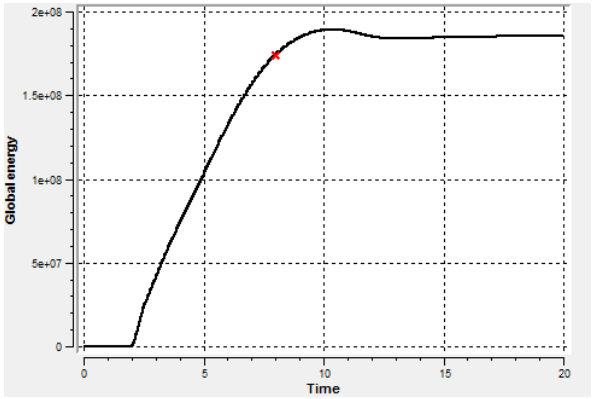


Figure 60: Global energy for ballast ship joint impact fixed at seabed

The horizontal velocity and acceleration in top of the tower is given in Figure 61. The acceleration peak is decreasing by excluding the soil from the simulation. Beyond this, the results are comparable to the case study.

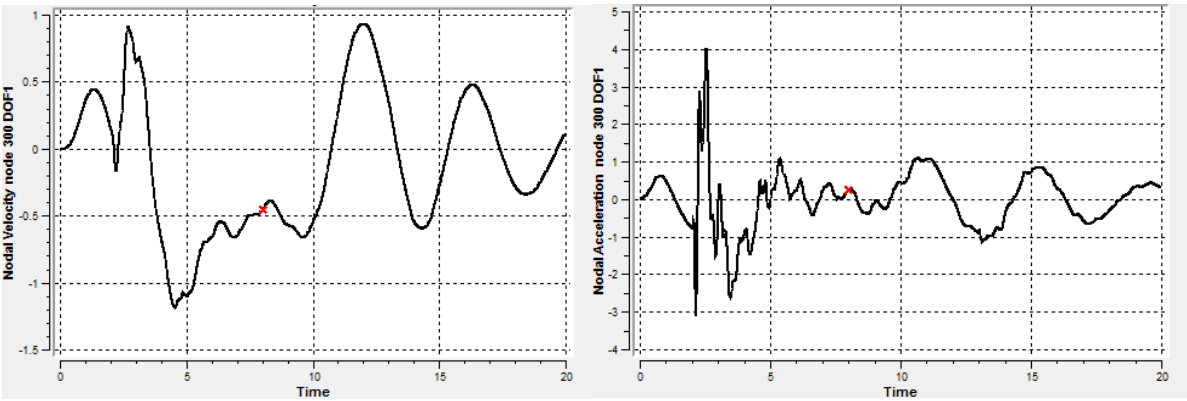


Figure 61: Velocity and acceleration in top of tower for ballast ship joint impact fixed at seabed

As observed from this analysis, the installation remains intact after the impact. However, large deformations are applied on the wind turbine. Practically, this might involve collapse of the structure that is not displayed in the numerical results.

### *Loaded ship column impact*

Contrary to the case with the loaded ship hitting the joint, impact with the column results in the fixed installation falling in the ship drifting direction, see Figure 62. The outcome of this impact is due to an early buckling of the leg on the opposite side of the impact. This contributes such that the wind turbine collapses away from the ship. Figure 63 shows an unsymmetrical motion of the nacelle during impact. The absorbed energy is given in Figure 64. The beginning of the horizontal translation is represented by a slope change in the global energy graph at approximately 5 s of simulation.

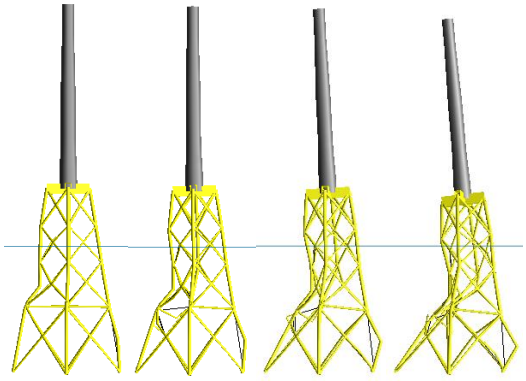

Figure 62: Failure pattern for loaded ship column impact fixed at seabed

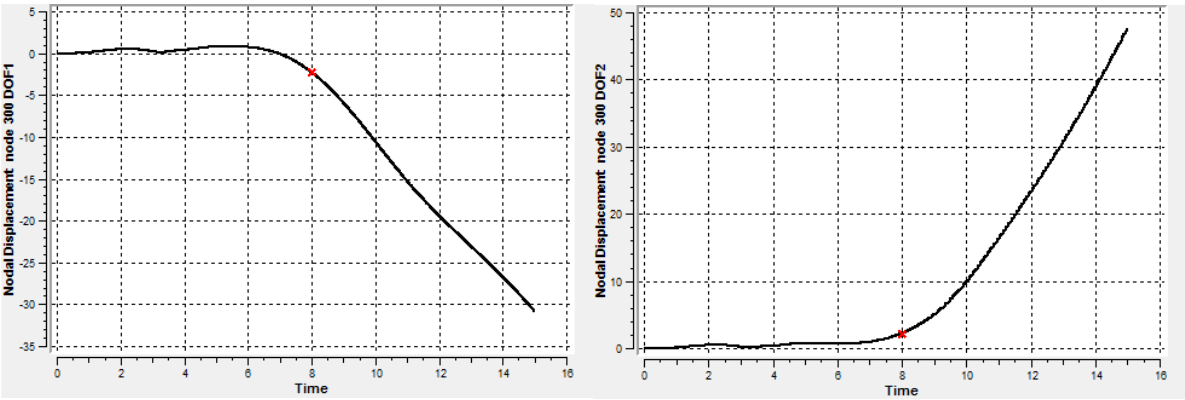


Figure 63: Displacement in top of tower for loaded ship column impact fixed at seabed

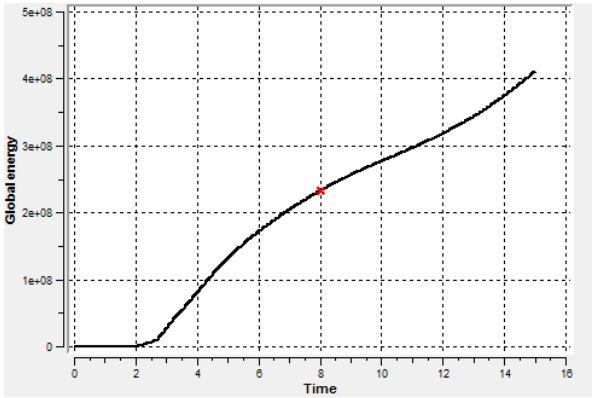


Figure 64: Global energy for loaded ship column impact fixed at seabed

The horizontal velocity and acceleration in the nacelle is given in Figure 65. The acceleration in top of the tower is comparable to the analysis including soil.

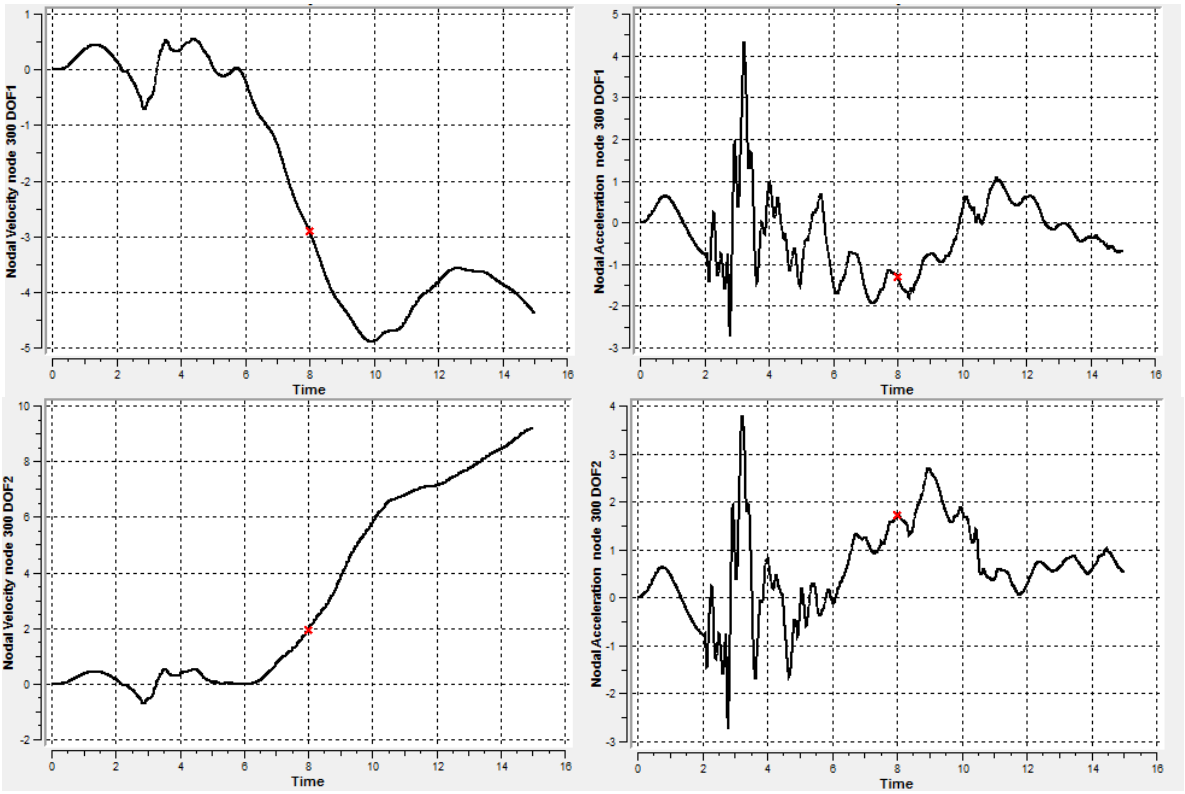


Figure 65: Velocity and acceleration in top of tower for loaded ship column impact fixed at seabed

### *Comments*

Conclusively, the importance of the soil condition is seen to be crucial. The weak upper layer causes a soft response of the installation and allows the jacket to move in the case studies results presented in Chapter 5. This prevents the structure from falling towards the ship. By fixing the jacket to the seabed, the 20 m deep impact results in the tower falling towards the ship. In this case, no buckling of the leg on the opposite side of the impact assists the jacket in falling away from the ship.

Significant changes in failure pattern occurred in all impact cases. Further investigation regarding the reliability of the soil parameters should be executed. In addition, due to large deformations in the analyses executed in this chapter, a larger part of the ship will be in contact with the jacket and a concentrated load is unrealistic.

No large compressive axial stresses are observed in any of the three impact cases. Local buckling causing the nacelle fixation fail is not considered a problem when assuming rigid soil.

## 6.1.2 Imperfection effect

The effect of the imperfection of 1.5 ‰ of the characteristic length is studied. This is done by first excluding the imperfection command from the dynamic analysis and afterwards increasing the imperfection to 5 ‰. By comparing the results to the one described in Chapter 5, no changes in the results are observed. Based on this, no major influence in structure strength is caused by including imperfections in the model. Perhaps larger imperfections affect the results. However, the goal with this sensitivity study is to verify the parameter used in the case study analyses, which seems reliable.

### 6.1.3 Elastic modulus of tower

In Section 3.2.3, the elastic modulus of the wind turbine tower is decreased from 2.1E5 to 0.84E5 MPa in order to prevent structural resonance. By running the analyses with the original value, the effect of the modification is studied. The horizontal acceleration for the loaded ship impacting both the joint and the column is shown in Figure 66. Comparing the graphs to the case study results, the peak acceleration decreases somewhat with a lower stiffness. In addition, the oscillations are reduced due to a stiffer response. However, the analyses show minor deviation due to the change. Conclusively, the modification is considered not to have large effect on the results.

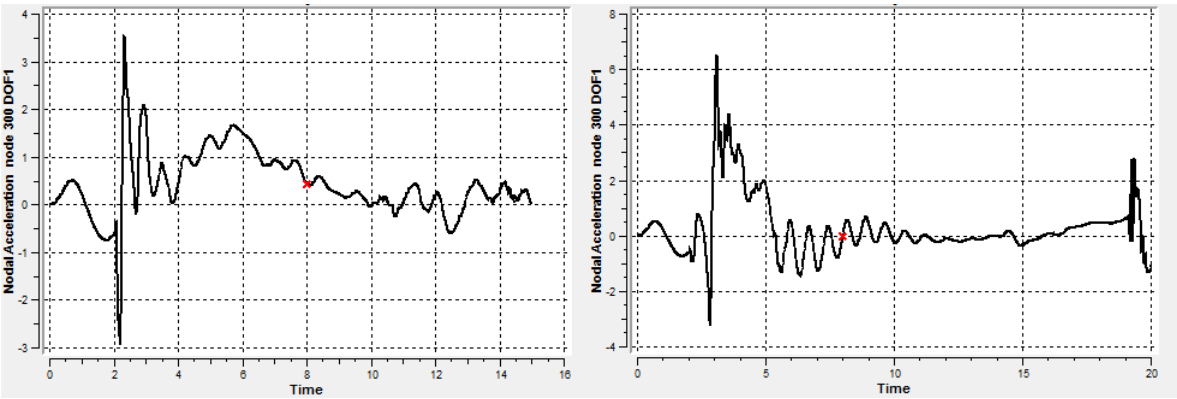


Figure 66: Acceleration in top of tower for loaded ship impact; Left: Joint, Right: Column

### 6.1.4 Local buckling

Local buckling of the tower can result in the installation falling over the ship and penetrating the deck. The calculation model described in Chapter 3 only includes beam elements. Local buckling is studied by using the buckling strength of 146 MPa, calculated in Section 4.3. The design buckling limit was exceeded in the analyses representing a loaded ship hitting the jacket between two joints and the ballast ship impact. In these cases, modelling of nonlinear shell elements accounting for dents and load redistribution will give more accurate results as shell elements allow out-of-plane buckling (Skallerud, 1998, Søreide et al., 1988). Due to the large computation time, only the lowest beam element in the tower is replaced.

The modelling of the beam-shell model is performed by Virtual Prototyping (Virtual Prototyping). The beam element is replaced by 16 shell elements in length direction and 60 in circular direction The element are formed as four-node, three-dimensional shell elements with the option QUADSHEL. They are 30 mm thick. The material corresponds to the rest of the tower; elastic modulus is 0.84E5 MPa, Poisson's ratio is 0.3, yield strength is 350 MPa and density is 7850 kg/m$^3$. A local dent is included in the middle of the element on the impact side of the tower. Additionally, the shell is given a curved shape with rotation in both ends pointing away from the ship. In order to increase the accuracy of the analyses, equilibrium iterations are included. The iterations ensure equilibrium between external and internal forces (USFOS, 2001). The option LITER includes one iteration. However, this increases the complexity of the system and the computational time.

The shell elements are connected to the beam elements in the tower and jacket foundation with elements comparable to spokes. This is shown in Figure 67, where some of the shell elements are removed in order to visualize the connection. The spokes are defined as riser beam elements formed as pipes with diameter of 3 m and thickness 30 mm. The function SURFPIPE visualizes the spokes with

diameter of 1 mm. The elastic modulus and Poisson's ratio for the spokes corresponds to the tower, while the yield strength and the density is 10 000 MPa and 7850E-6 kg/m$^3$, respectively.

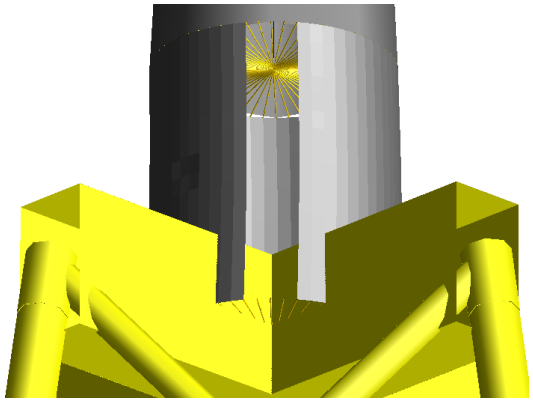

Figure 67: Spoke elements connecting shell to beam

In order to check whether the shell elements allow the tower to buckle, buckling is provoked by decreasing the shell thickness from 30 to 10 mm. Only the ballasted and loaded inter-joint ship impact cases are evaluated, where the results in Chapter 5 show large compressive forces on the hit side of the tower. The plastic node utilization using thin shells is shown in Figure 68, ballast condition to the left and loaded ship impact to the right. The horizontal acceleration in top of the tower is given in Figure 69. As seen, buckling occurs on the impact side of the wind turbine tower. The buckling develops during the first peak in the acceleration, as expected. However, due to the relatively small thickness, rather low accelerations cause local buckling.

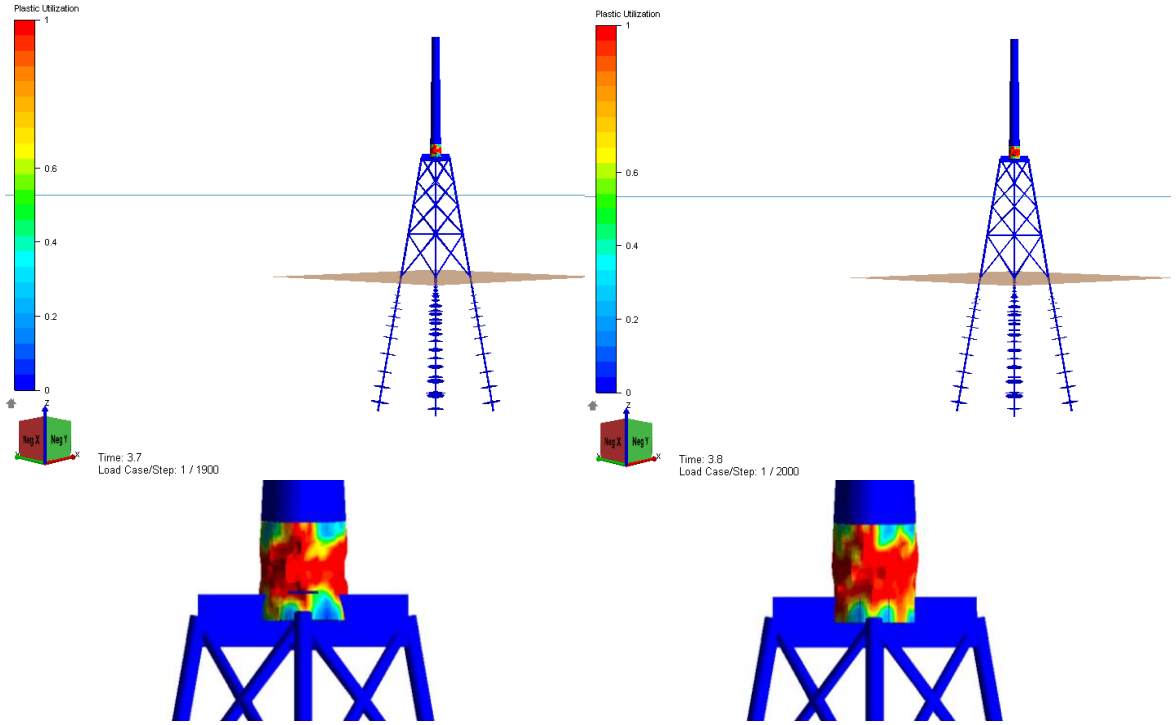


Figure 68: Plastic utilization including 10 mm shell elements; Left: Ballast, Right: Loaded

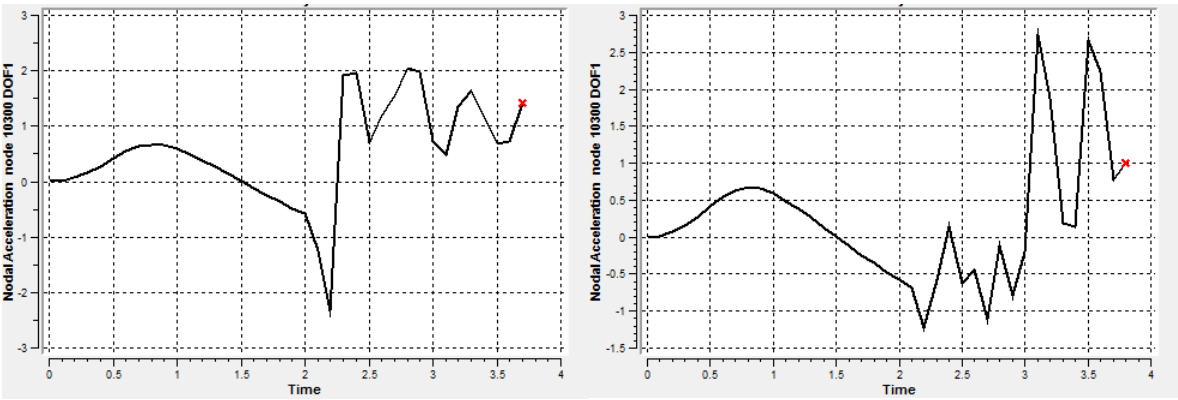


Figure 69: Acceleration in top of tower including 10 mm shell element; Left: Ballast, Right: Loaded

Using the original thickness of 30 mm in the shell elements, the probability of local buckling in the tower during a ship collision is evaluated in the following.

### *Ballast ship joint impact*

The collapse pattern for impact between a ballasted ship and a jacket supported wind turbine is shown in Figure 70. The installation withstands the collision. As seen, outwards buckling of the leg replaces the inwards buckling observed in the case study results. Based on the horizontal displacement and acceleration graph from the upper node in the tower in Figure 71 and Figure 72, equilibrium is reach at an earlier stage of the simulation. The resulting displacement of the tower and global energy is lower.

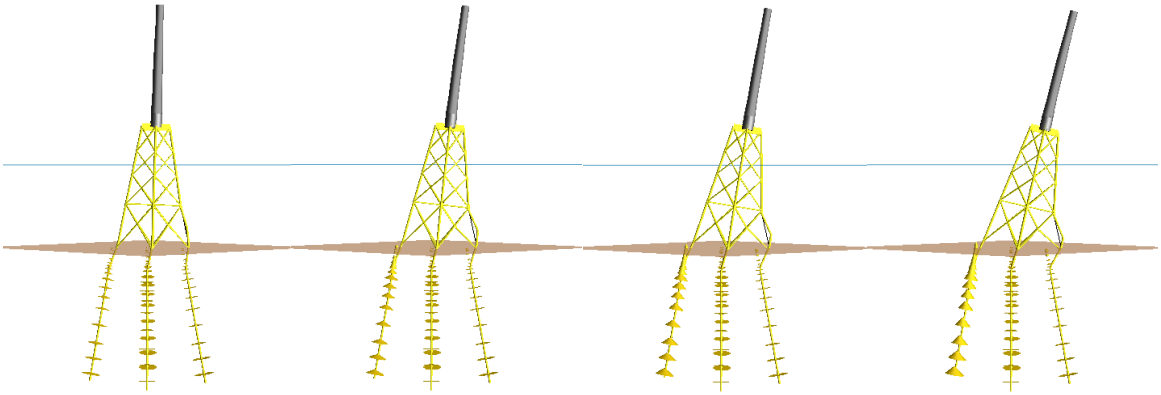

Figure 70: Failure pattern for ballast ship joint impact including shell element

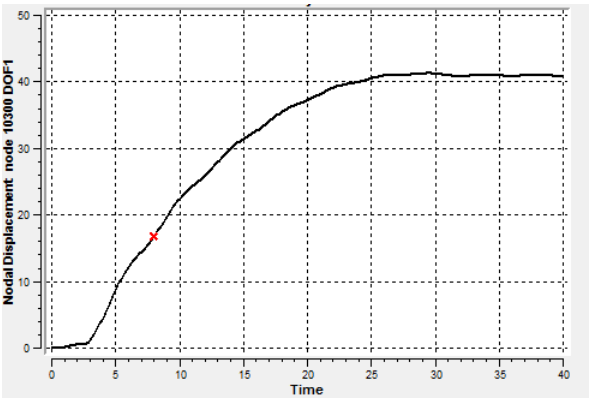


Figure 71: Displacement in top of tower for ballast ship joint impact including shell element

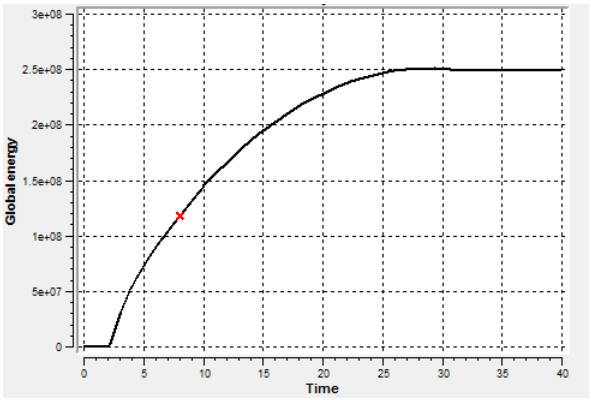


Figure 72: Global energy for ballast ship joint impact including shell element

In order to evaluate buckling of the tower, the plastic utilization of the nodes is studied. The maximum plastic utilization of the shell nodes during the whole analysis is given in Figure 73. This occurred during the peak horizontal acceleration in top of the tower at the beginning of the impact. As observed from the color range, the tower is far away from experiencing local buckling with 30 mm thick walls.

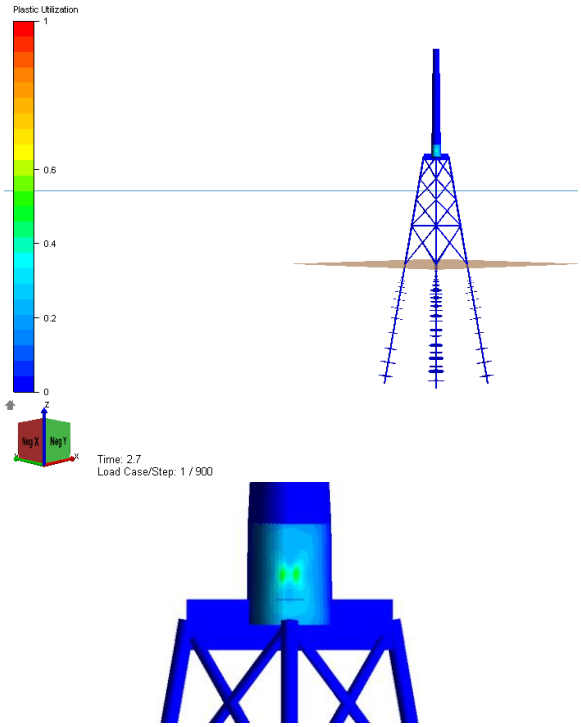


Figure 73: Plastic utilization for ballast ship joint impact including shell element

## *Loaded ship column impact*

The collapse pattern for the loaded ship inter-joint impact shown in Figure 74 corresponds to the figures presented in Section 5.2.2. The horizontal displacement in top of the tower is given in Figure 75 and the global energy in Figure 76. Both figures show that the collapse is less developed within the 20 s of simulation.

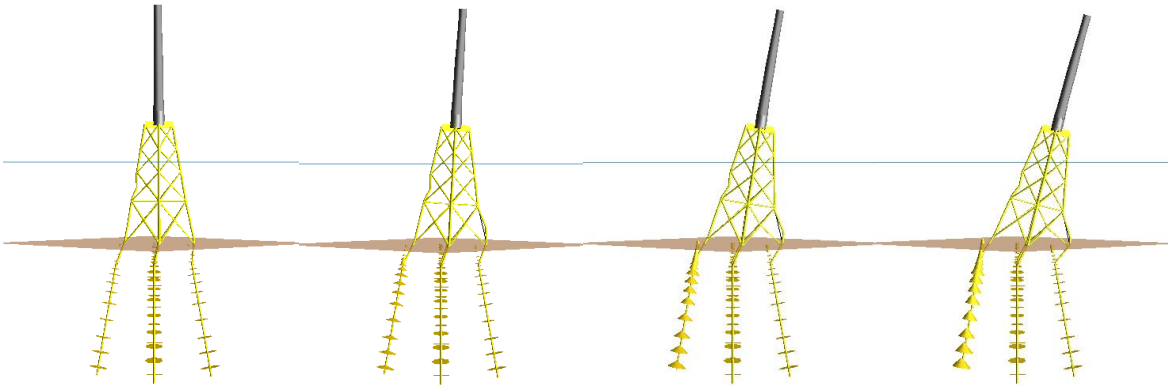

Figure 74: Failure pattern for loaded ship column impact including shell element

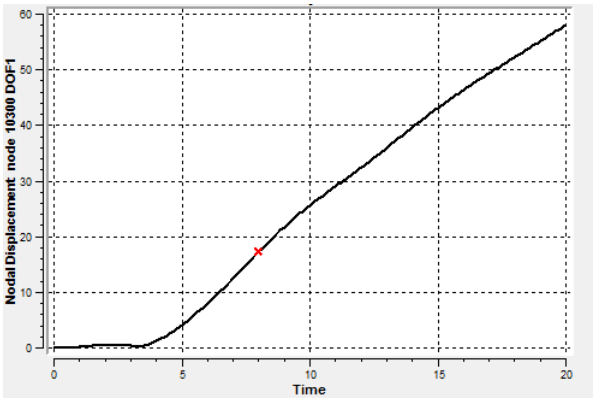


Figure 75: Displacement in top of tower for loaded ship column impact including shell element

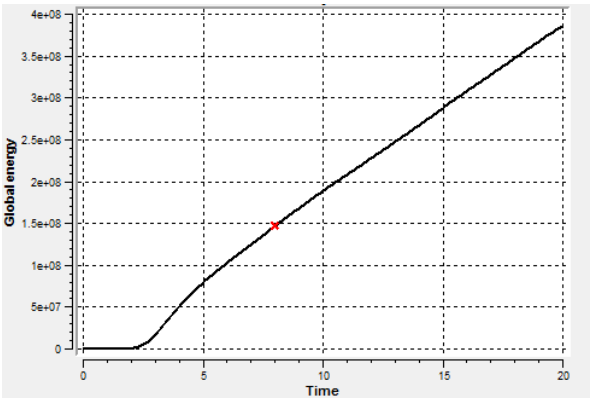


Figure 76: Global energy for loaded ship column impact including shell element

The maximum plastic utilization in the shell nodes during the impact is given in Figure 77. As seen, the maximum value is well below the plasticity limit, indicating no local buckling of the tower.

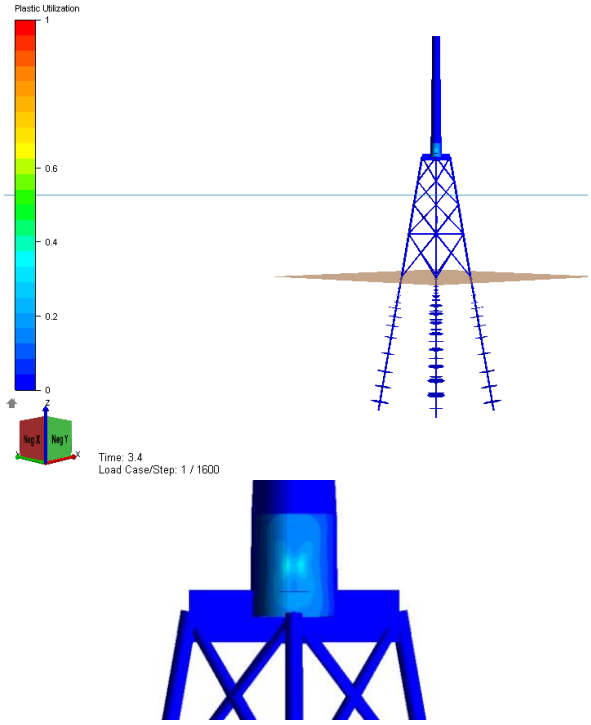


Figure 77: Plastic shell nodes utilization for loaded ship column impact including shell element

### *Comments*

Conclusively, no local buckling due to a large oil tanker drifting into the offshore wind turbine is present. The tower falling towards the ship due to large inertia is assumed not to be a problem. The results from this section indicate that the calculated buckling strength of 146 MPa might be conservative.

## 6.2 Ship impact velocity

The ship velocity of 2 m/s is based on standard event for ships drifting due to loss of engine power, both stated in BSH and DNV wind turbine standards. This sensitivity study of varying the impact velocity is performed due to the interest of evaluating the influence of this parameter.

By increasing the velocity from 2 to 3 m/s, the displacement and acceleration in top of the tower is increased. All three impact cases results in the wind turbine not being able to dissipate the kinetic energy from the ship and collapsing away from the ship, including the ballast ship impact. Figure 78 shows the collapse development of the loaded ship hitting the jacket between two joints. The collapse of the wind turbine develops faster as the velocity is increased. The increased drifting speed cause larger peak acceleration, see Figure 79, which again cause larger compressive forces in the tower on the impact side, see Figure 80.

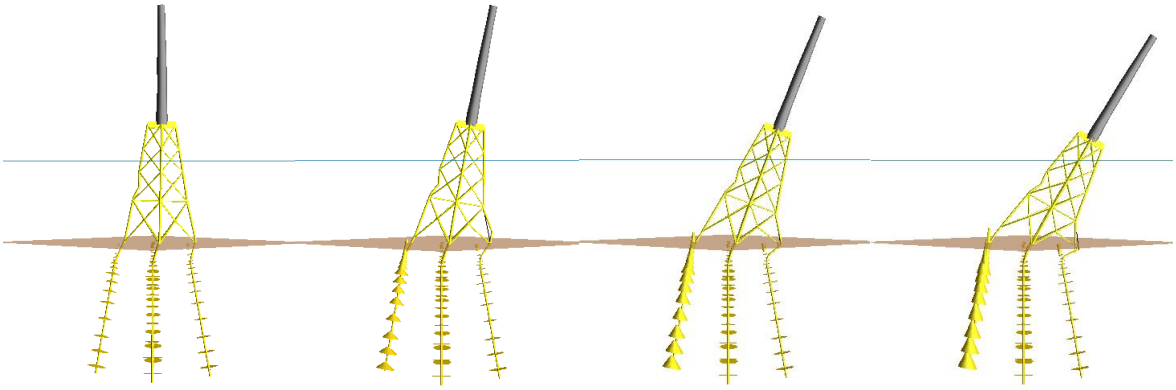

Figure 78: Failure pattern for loaded ship column impact drifting 3 m/s

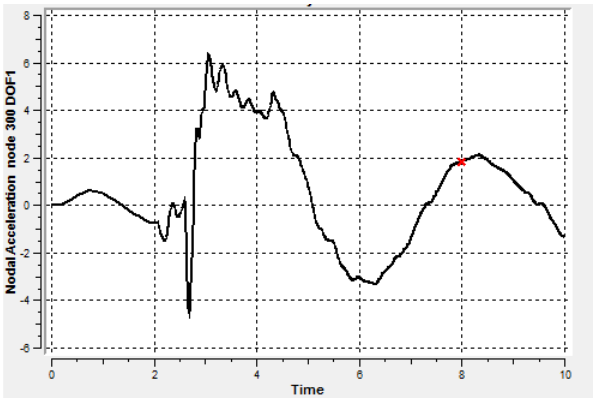


Figure 79: Acceleration in top of tower for loaded ship column impact drifting 3 m/s

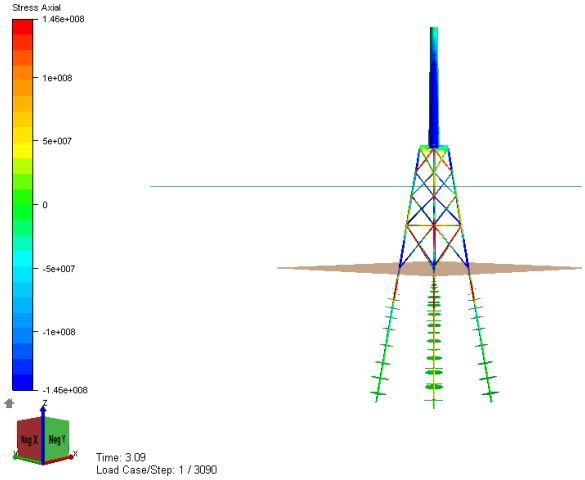


Figure 80: Axial stress for loaded ship column impact drifting 3 m/s

A reduction in the ship velocity to 1 m/s gives the opposite results. In all impact cases, the installation absorbs the energy and withstands the impact. The failure pattern of the installation due to the loaded ship column impact is given in Figure 81. No buckling of the jacket leg on the opposite side of the impact is present. The acceleration in top of the tower decreases and the axial stress is within the allowable limit for local buckling, see Figure 82 and Figure 83.

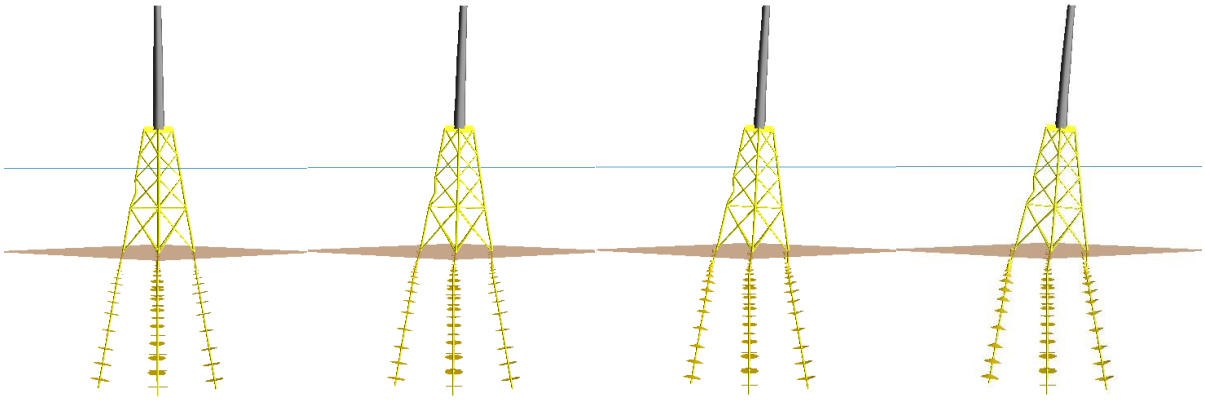

Figure 81: Failure pattern for loaded ship column impact drifting 1 m/s

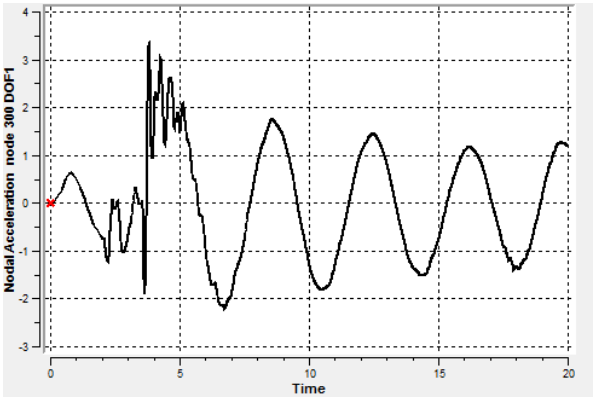


Figure 82: Acceleration in top of tower for loaded ship column impact drifting 1 m/s

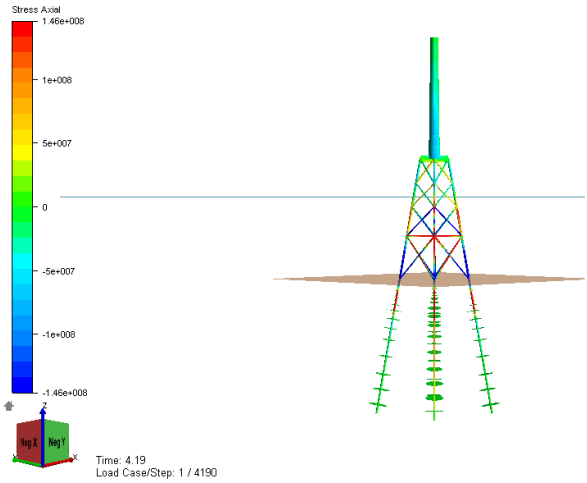


Figure 83: Axial stress for loaded ship column impact drifting 1 m/s

## 6.3 Forces

### 6.3.1 Closed down energy production

The thrust force is acting in the ship drifting direction and is contributing such that the offshore wind turbine is falling away from the ship. Closed down energy production is less favourable considering the

collapse direction. Assuming an acceleration of 5 m/s$^2$ in top of the tower, the horizontal force contributions due to the weight of the turbine and the thrust force are;

$$F_{weight} = m \cdot a = 350 \cdot 10^3 \cdot 5 = 1.75\ MN \tag{31}$$

$$F_{thrust} = 0.5\ MN \tag{32}$$

where $m$ is the weight of the turbine and $a$ is the acceleration. According to these calculations, the thrust is responsible for a significant part of the horizontal forces in top of the tower. In order to study global motion of the installation during a ship collision when closed down, the thrust force is excluded from the analyses.

Considering the loaded ship joint impact without the thrust force, the tower experience less displacement and the global energy is decreased, see Figure 84 and Figure 85. Some increase in the peak acceleration in top of the tower at the beginning of the analysis due to the inertia forces from the turbine is observed, see Figure 87. This causes an increased compressive force on the ship side of the wind turbine tower. However, the critical limit of 146 MPa is not exceeded, see Figure 86. The two other impact cases still have significant compression on the hit side at the beginning of the impact.

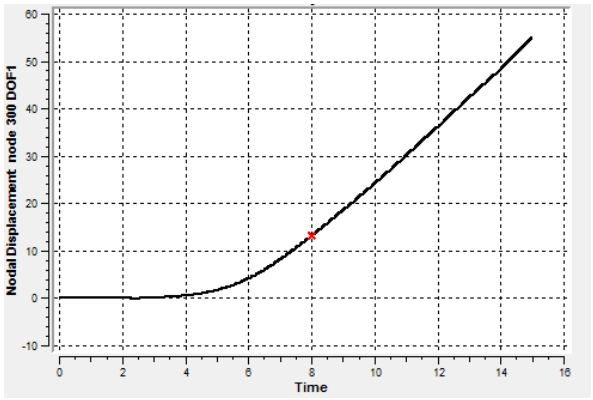


Figure 84: Displacement in top of tower for loaded ship joint impact with no thrust

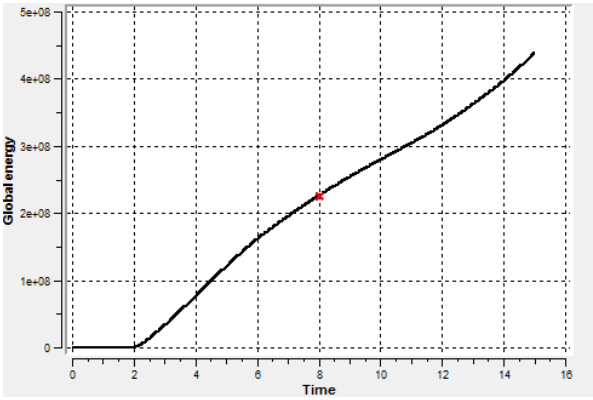


Figure 85: Global energy for loaded ship joint impact with no thrust

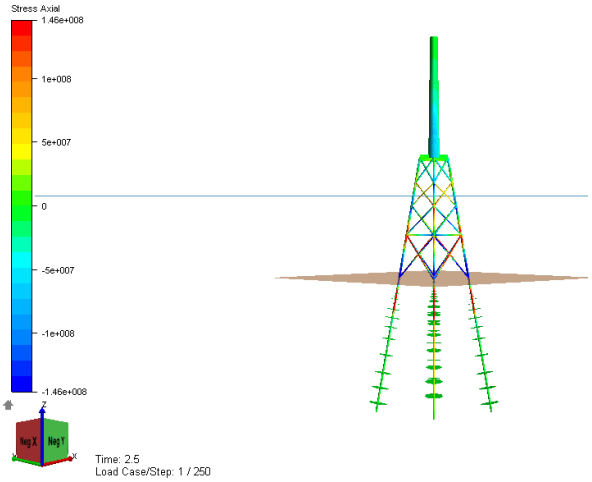


Figure 86: Axial stress for loaded ship joint impact with no thrust

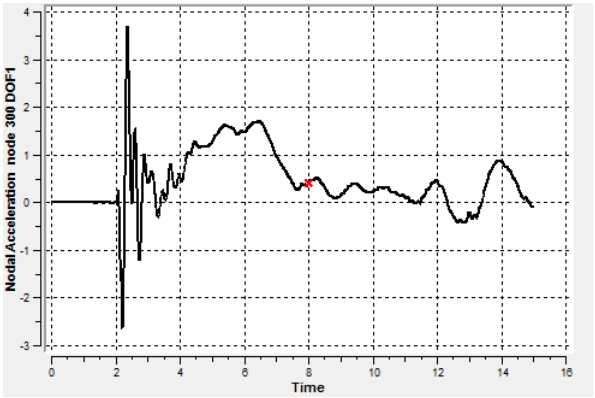


Figure 87: Acceleration in top of tower for loaded ship joint impact with no thrust

Conclusively, the thrust force is not significantly affecting the outcome of the global response of the installation due to ship collision. It is not the main reason causing the tower to collapse away from the ship and only contributes in a minor part to the failure pattern. However, minor increase in the possibility for local buckling of the tower is observed when closing town the energy production.

### 6.3.2 Hydrodynamic forces

The case studies include hydrodynamics through the option WAVEDATA. The influence of these hydrodynamic forces is studies by excluding WAVEDATA from the analyses. For the two loaded cases, no significant changes in the results are observed. However, for the ballast ship impact, the installation is no longer able to withstand the impact and collapses away from the ship. The failure pattern in Figure 88 is comparable to the case study results given in Section 5.2.2. The displacement of the nacelle in Figure 89 and the global energy in Figure 90 indicates that the structure collapses. Based on this, the drag forces and added mass is demonstrated to damp the overturning of the wind turbine.

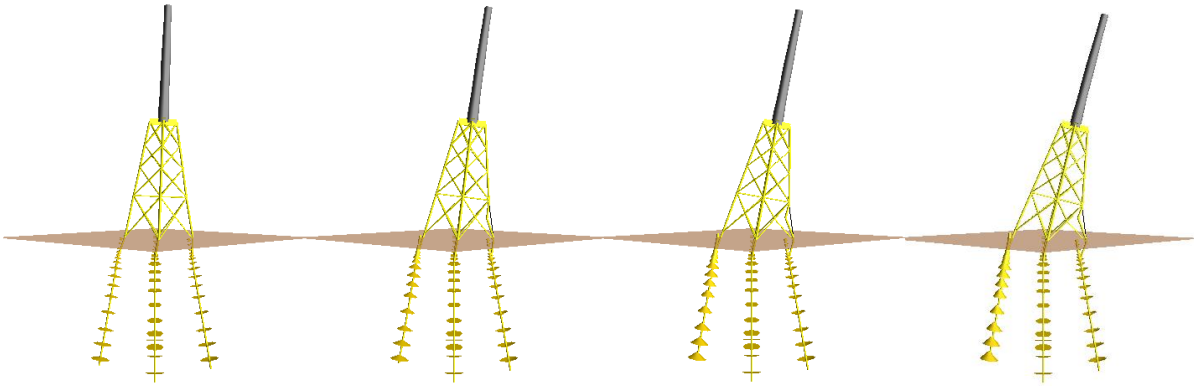

Figure 88: Failure pattern for ballast ship joint impact without hydrodynamics

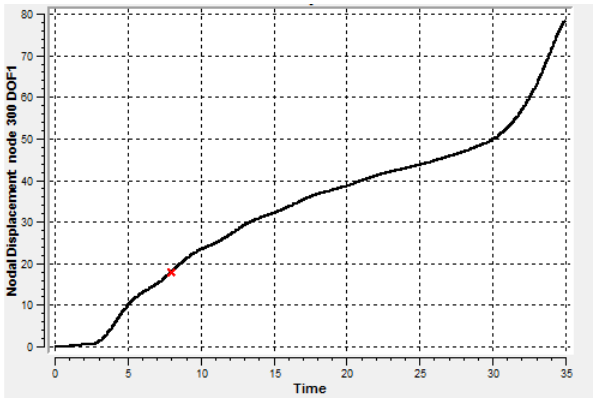


Figure 89: Displacement in top of tower for ballast ship joint impact without hydrodynamics

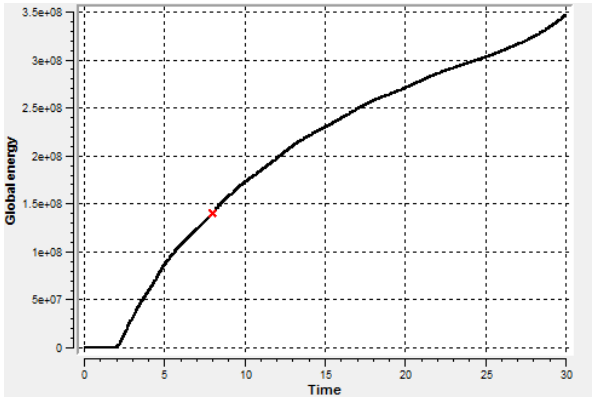


Figure 90: Global energy for ballast ship joint impact without hydrodynamics

# Chapter

# 7. Conclusion and recommendations for further work

The main goal with this work is to study the possibility of achieving the design check in the BSH standard "Design of Offshore Wind Turbines". The standard requires more than 500 MJ in collision energy due to impact between an oil tanker and jacket wind turbine. BSH states that risk analysis must demonstrate that either the collision energy is absorbed by the structures or results in offshore wind turbine collapse without damaging the ship hull.

Environmental pollution due to oil spill from the tanker as an outcome of the collision is evaluated in this research. Both failure due to overall deformation of the installation and local damage of the tower is studies. In addition, failure of the nacelle fixation is investigated.

The impact study is executed with nonlinear static and dynamic analyses in the software USFOS. The offshore wind turbine model is received from Virtual Prototyping. The ship-jacket contact is modelled as concentrated force through a nonlinear spring. The case studies include an infinitely rigid ship, not contributing to dissipate the impact energy. The numerical simulation is based on beam theory. Three different impact cases are studied; a loaded ship with 532 MJ impact energy hitting the jacket at 20 or 12.5 m below the sea surface and ballasted ship with energy of 196 MJ impacting at 5 m depth. The loaded ship impact is of major interest in this research due to the possibility of oil spill.

## 7.1 Conclusion

The results from the case studies presented in Chapter 5 show that the response of the offshore wind turbine is favourable for the ship. Seen from the global energy graphs, the wind turbine is not capable of absorbing the design energy required by BSH. The installation do not withstand an impact with a loaded ship of 160 000 dwt. The response of the installation is soft and both the jacket and the tower collapse away from the ship. Depending on impact case, lateral – and axial failure develops. The failure sometimes involves buckling of the jacket leg on the opposite side of the impact. The bolts securing the nacelle to the tower are given a critical acceleration of 1 G. None of the acceleration graphs from the analyses exceed this limit and bolt failure is assumed unlikely. Based on this, BSH consider the wind turbine analysed in this work as "collision friendly".

However, the required design energy involves large inertia, possibly causing local buckling and unfavourable failure of the tower towards the ship. As the FEA is based on beam theory, local buckling is not included. By using hand calculations including shell theory, out-of-plane buckling is studied. The buckling strength is calculated to be 146 MPa. The axial stress screenshots are scaled according to this value. The impact with the loaded 160 000 dwt tanker at 12.5 m depth and the ballast ship impact are observed to involve large compression on the impact side of the tower in the early stage of the collision.

More accurate verification of these compressive forces is performed by including shell theory in the FEA. The lowest beam element in the tower is replaced with shell elements. The results show no sign of local buckling. Based on this, the buckling strength of 146 MPa might be over-conservative. Conclusively, the tower falling towards the ship, causing the nacelle hitting the deck and penetrating the cargo tanks, is not of concern.

In order to verify the obtained results, sensitivity studies of the analyses are executed. Different parameters are varied and the influence is studied. Most of the parameters do not affect the outcome significantly. However, interesting results are observed from the soil study. The case study results demonstrate failure in the soil due to a weak upper layer. The weak soil introduces a soft response of the jacket. The affection of the soil is studied by fixing the jacket to the seabed. This replaces soil failure with failure in the jacket. The inter-joint impact at 12.5 m depth still results in the wind turbine collapsing in the drifting direction of the ship. However, impact at 20 m depth results in the nacelle moving in the ship direction possibly hitting the ship deck and penetrating the cargo tanks. The 20 m deep impact is the only failure without buckling of the leg on the opposite side of the impact. Based on this, the leg buckling assists the installation in collapsing into the sea in the drift direction of the ship. On the other hand, the compression in the tower on the hit side when fixing the jacket to the seabed is decreased compared to the case study results. Based on this, local buckling is not considered a problem. These analyses show that the importance of the soil parameters is crucial. The soil condition used in this work prevents the structure from collapsing towards the ship.

Based on the structural and environmental assumptions made during this research, negative influence of failures on the impact side of the offshore wind turbine is not considered a problem. Major environmental pollution is assumed not to occur due to an impact between a 160 000 dwt oil tanker and offshore jacket wind turbine. The installation is collapsing away from the ship. In addition, neither the tower nor the nacelle is observed falling in the ship direction due to large inertia. The requirement from BSH seems to be satisfied and the FE wind turbine model does not need any modifications in order to avoid oil spill as suggested in the assignment.

## 7.2 Recommendations for further work

The model used in this work is based on beam theory. As stated in the assignment, significant compressive forces in the wind turbine are present during a ship collision. This might include out-of-plane buckling of the tower, which is not displayed with beam elements. In order to account for this, the lower beam element in the wind turbine tower is replaced by shell elements. Large compressive forces are observed in large parts of the hit side of the tower in the early stages of impact. Based on this, shell elements in a larger part of the model might give a more accurate model considering local buckling. However, this will require longer computational time.

The influence of the soil characteristics is proven to be crucial. Based on information from Virtual Prototyping, the given quantities used in this research is to be representative for offshore wind turbine development in the North Sea. However, in order to validate the results presented in this report, further investigation of the input values should be conducted. In addition, specific values for a given location should be used when deciding to build a wind farm and performing risk analysis.

Nonlinear, compressive springs represent the contact between the ship and the offshore wind turbine. Ductility design principle is used and the ship is modelled to be rigid. This involves that no energy is absorbed by the ship and the kinetic impact energy is dissipated as kinetic and strain energy in the wind turbine. In reality, the ship will absorb some energy. This might be introduced by including dash-pots in the contact representation.

The ship-jacket impact is described as a concentrated load. This is a conservative assumption, as the ship in reality would impact a larger part of the jacket when the jacket deforms. During the wind turbine

collapse, the impact location will change as the ship remains in its vertical position and therefore is sliding along the installation. Further study within the representation of the impact description should be conducted.

In this research, ship incoming 45° counter-clockwise on the positive x-axis hitting one jacket leg is studied. However, the ship might drift into the wind turbine hitting either two legs or impact with the cross-bracings. This assignment is based on the BSH standard design check, of which involves sideways drift of a ship into the wind farm. Whether other drifting patterns involves different outcome is not investigated in this research, however, should be evaluated.

Two different impact locations are studied for the loaded ship condition. One of them is located at 20 m below the sea surface. This depth is below the level normally considered exposed to ship impact. The results from this impact case stands out compared to the other impact cases. Following by the sensitivity study when excluding the soil from the analyses and fixing the jacket to the seabed, this is the critical impact location causing the installation to collapse towards the ship. Based on this, recommendations and design aspects should not only rely on the results from this specific impact.

# References

AMDAHL, J. 1991. *Consequences of ship collisions,* London, Royal Institution of Naval Architects.
AMDAHL, J. 2005. *TMR4205 - Buckling and Ultimate Strength of Marine Structures,* Trondheim.
AMDAHL, J. & EBERG, E. 1993. *Ship collision with offshore structures,* Rotterdam, Balkema.
AMDAHL, J., HOLMÅS, T., HELLAN, Ø. & EBERG, E. USFOS.
AMDAHL, J. & JOHANSEN, A. 2001. *High-energy ship collision with jacket legs,* [S.l.], [s.n.].
BARD, J. 2010. *ORECCA; Offshore, Renewable Energy, Conversion platforms, Coordination Action* [Online]. supergen-marine. Available: http://www.supergen-marine.org.uk/drupal/files/events/assembly_2010_presentations/guests/bard_2010_orecca.pdf [Accessed 16.02.2011 2011].
BARLTROP, N. D. P. & ADAMS, A. J. 1991. *Dynamics of fixed marine structures,* Oxford, Butterworth-Heinemann.
BIEHL, F. 2004. *Rechnerische Bewertung von Fundamenten von Offshore Windenergieanlagen bei Kollisionen mit Schiffen,* Hamburg, Arbeitsbereiche Schiffbau der Technischen Universität Hamburg-Harburg.
BIEHL, F. & LEHMANN, E. Year. Collisions of Ships with Offshore Wind Turbines: Calculation and Risk Evaluation. *In:* International Conference on Collision and Grounding of Ships, 4th, 2007 Hamburg, Germany. 55-61.
BSH 2007. Design of Offshore Wind Turbines. Hamburg and Rostock.
BWEA 2005. BWEA Briefing Sheet: Wind Turbine Technology. London.
DALHOFF, P. & BIEHL, F. 2005. Ship Collision, Risk analysis - Emergency systems - Collision dynamics. Hamburg, Germany: Germanisher Lloyd WindEnergie GmbH and Hamburg University of Technology.
DNV 2002. DNV-RP-C202; Buckling strength of shells.
DNV 2004. DNV-RP-C204; Design Against Accidental Loads. *Ship Collisions.*
DNV 2007. Design of offshore wind turbine structures.
EEA 2009. Europe's onshore and offshore wind energy potential - An assessment of environmental and economic constraints. Copenhagen.
ELLIS, J., FORSMAN, B., HÜFFMEIER, J. & JOHANSSON, J. 2008. Methodology for Assessing Risks to Ship Traffic from Offshore Wind Farms. Göteborg, Sweden: SSPA Sweden AB.
EWEA Factsheet: Offshore.
EWEA 2011a. The European offshore wind industry key trends and statistics 2010.
EWEA 2011b. Statistics: Operational Offshore Wind Farms end 2010.
HAVER, S. K. 2011. Prediction of Characteristic Response for Design Purposes. Statoil.
HOLMÅS, T. 1999. Release Notes: USFOS Version 7-6. 7-6 ed. Trondheim: SINTEF Structural Engineering.
IMO 2004. Regulations for carriage of AIS.
MOAN, T. 2003. *TMR 4190 - Finite Element Modelling and Analysis of Marine Structures,* Trondheim.
MORISON, J. R., O'BRIEN, M. P., JOHNSON, J. W. & SCHAAF, S. A. 1950. The force exerted by surface waves on piles. *Petroleum Transactions,* 189**,** 149-154.
NIELSEN, F. G. 2006. Presentasjon: Kan vindmøller installeres til havs? Bergen: NTVA.
NORSOK 2004a. N-001: Structural design.
NORSOK 2004b. N-004: Design of steel structures. *Annex A: Design against accidental actions.*
NORSOK 2007. N-003: Actions and action effects. *10.2.5.5: Air gap analysis.*
NPD 1985. *Regulation for Structural Design of Load-bearing Structures Intended for Exploitation of Petroleum Resources,* Oslo, NPD.

OFFSHOREWIND.NET. 2009. *Offshore Wind Turbine Foudations - Current & Future Prototypes* [Online]. Available: http://offshorewind.net/Other_Pages/Turbine-Foundations.html [Accessed 16.02.2011 2011].

SKALLERUD, B. 1998. Shell Element Theory: Efficient stress resultant placticity formulation for thin shell applications: Implementation and numerical tests. Trondheim: SINTEF

SØREIDE, T. H. 1981. *Ultimate load analysis of marine structures,* [Trondheim], Tapir.

SØREIDE, T. H., AMDAHL, J., EBERG, E., HOLMÅS, T. & HELLAN, Ø. 1988. USFOS - A Computer Program for Progressive Collapse Analysis of Steel Offshore Structures. Theory Manual. SINTEF.

USFOS 2001. USFOS Getting Started. SINTEF GROUP.

USFOS 2010. USFOS USER'S MANUAL: Input Description USFOS Control Parameters.

VIRTUAL PROTOTYPING USFOS offshore wind turbine model.

WWW.JPFIL.COM. Available: http://www.jpfil.com/vasf/scenesquebec/navires.htm [Accessed 21.02.2011 2011].

WWW.MARINETRAFFIC.COM. 2011. *Cap Diamant* [Online]. Department of Product & Systems Design Engineering - University of the Aegean. Available: http://www.marinetraffic.com/ais/shipdetails.aspx?MMSI=239876000 [Accessed 16.02.2011 2011].

# Bibliography

BERGE, S. 2006. *Fatigue and fracture design of marine structures,* Trondheim, Marinteknisk senter.

BIEHL, F. & LEHMANN, E. 2005. Collisions of Ships with Offshore Wind Turbines: Calculation and Risk Evaluation. *In:* KÖLLER, J., KÖPPEL, J. & PETERS, W. (eds.) *Offshore Wind Energy - Research on Environmental Impacts.* Berlin: Springer-Verlag.

DEN BOON, H., JUST, H., HANSEN, P. F., RAVN, E. S., FROUWS, K., OTTO, S., DALHOFF, P., STEIN, J., VAN DER TAK, C. & VAN ROOIJ, J. 2005. Reduction of Ship Collision Risks for Offshore Wind Farms - SAFESHIP.

FALTINSEN, O. M. 1999. *Sea loads on ships and offshore structures,* Seoul, Society of Naval Architects of Korea.

IRGENS, F. 1999. *Formelsamling mekanikk: statikk, fasthetslære, dynamikk, fluidmekanikk,* Trondheim, Tapir.

MARTIN, G. & ROUX, J. 2010. *Wind turbines: types, economics and development,* New York, Nova Science.

PENG, L. 2010. *Analysis and Design of Offshore Jacket Wind Turbine.* Master Degree Master Thesis, Norwegian University of Science and Technology.

PETTERSEN, B. 2007. *Marin teknikk 3: hydrodynamikk,* Trondheim, Marinteknisk senter.

VISSER, W. 1993. *The structural design of offshore jackets,* London, The Marine Technology Directorate Limited.

# Appendices

## A. Results from case studies

### *Static: Loaded ship joint impact*

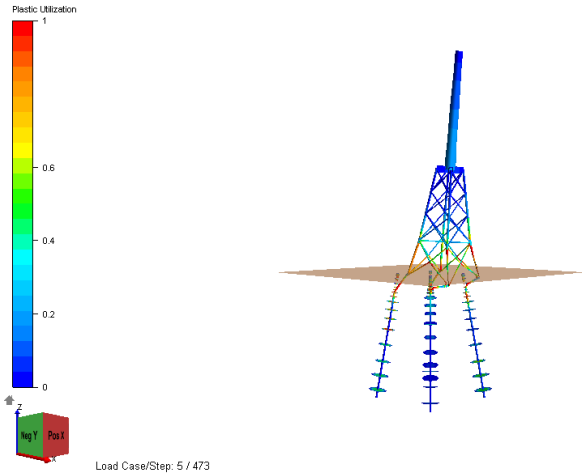


Static plastic utilization for loaded ship joint impact

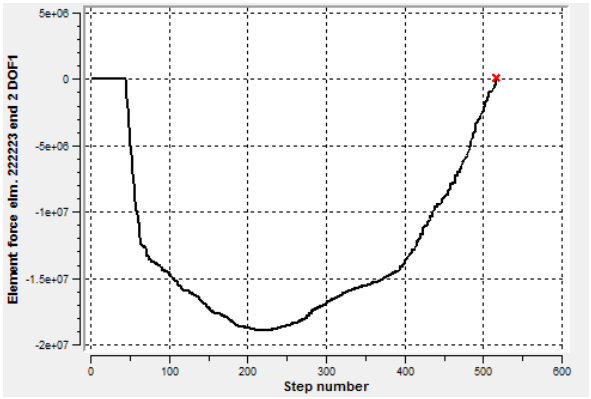


Static spring force for loaded ship joint impact

### *Static: Ballast ship joint impact*

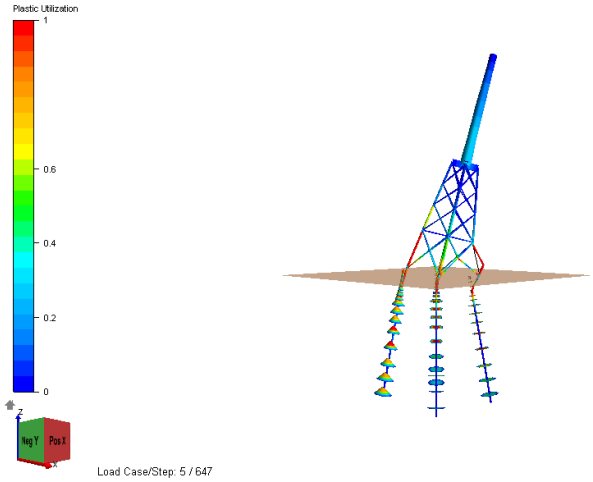


Static plastic utilization for ballast ship joint impact

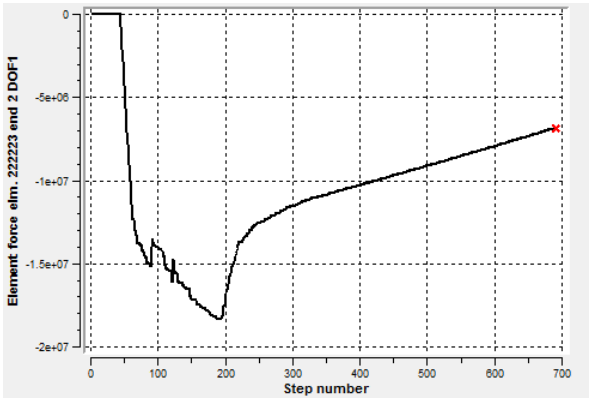


Static spring force for ballast ship joint impact

### *Static: Loaded ship column impact*

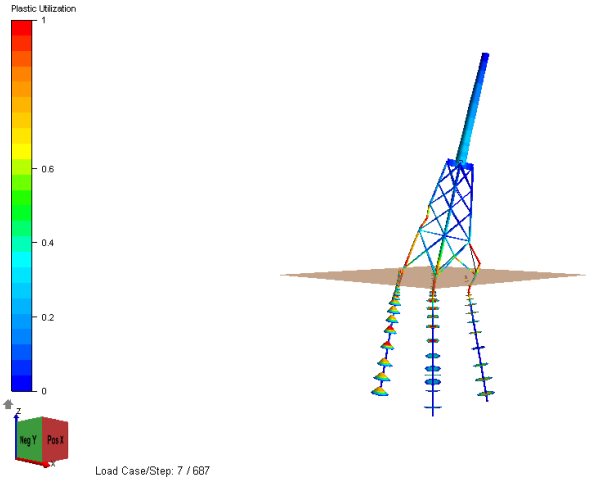


Static plastic utilization for ballast ship joint impact

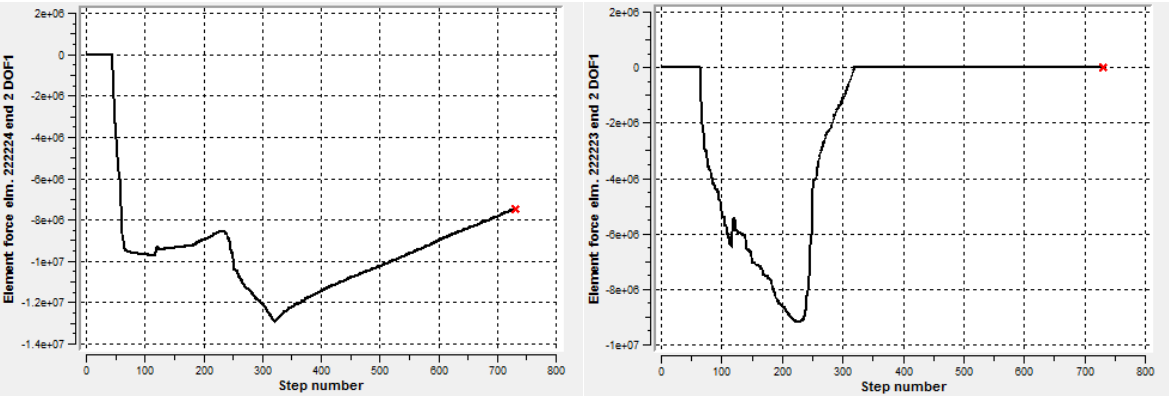


Static spring force for ballast ship joint impact

### *Dynamic: Loaded ship joint impact*

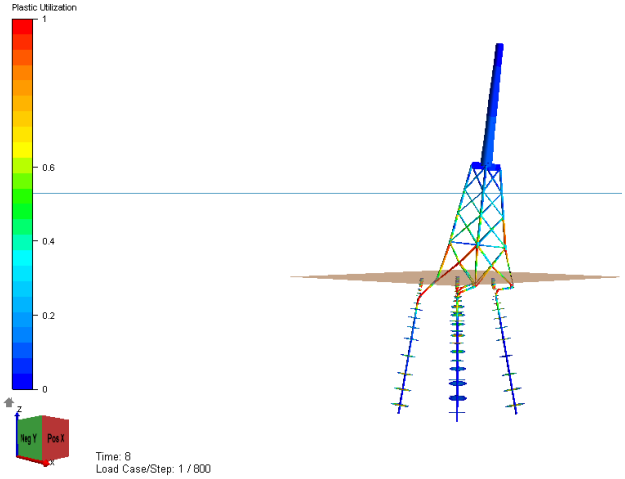


Dynamic plastic utilization for loaded ship joint impact

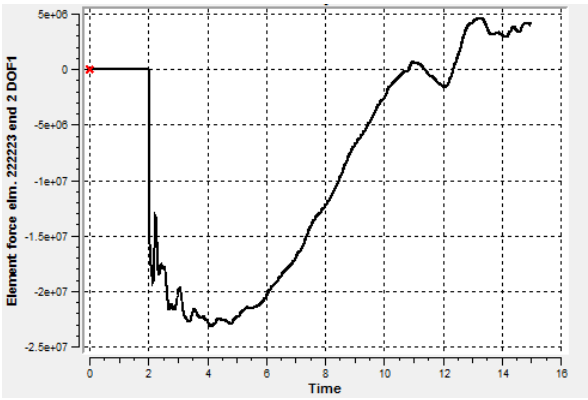


Dynamic spring force for loaded ship joint impact

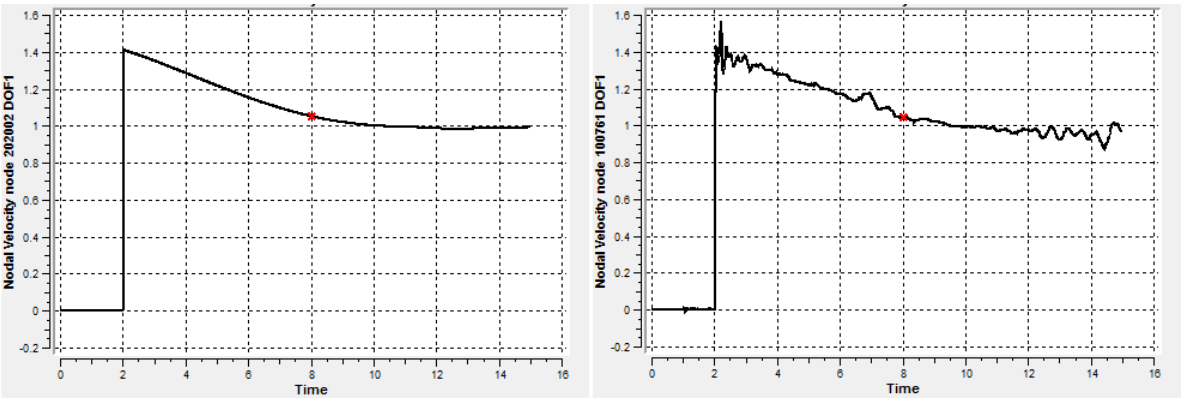


Dynamic ship velocity and velocity in impact node for loaded ship joint impact

### *Dynamic: Ballast ship joint impact*

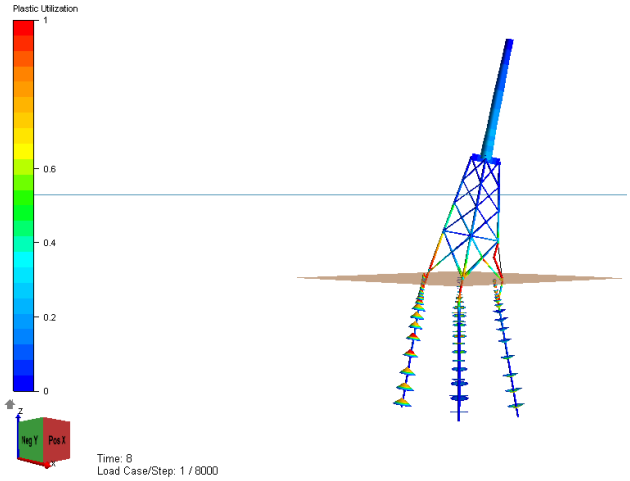


Dynamic plastic utilization for ballast ship joint impact

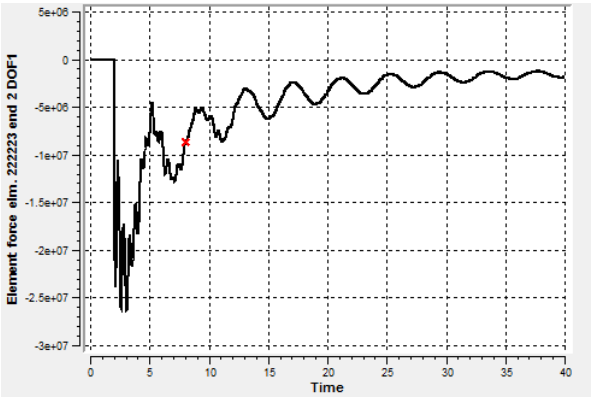


Dynamic spring force for ballast ship joint impact

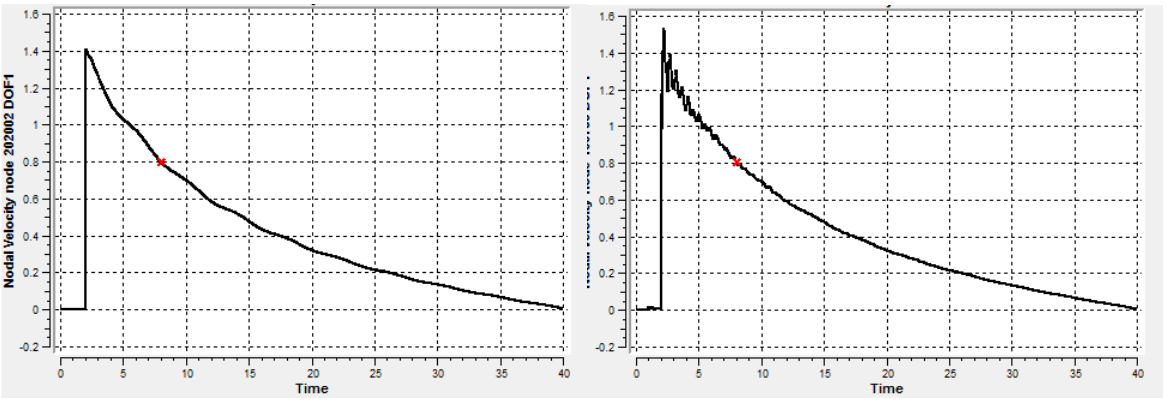


Dynamic ship velocity and velocity in impact node for ballast ship joint impact

### *Dynamic: Loaded ship column impact*

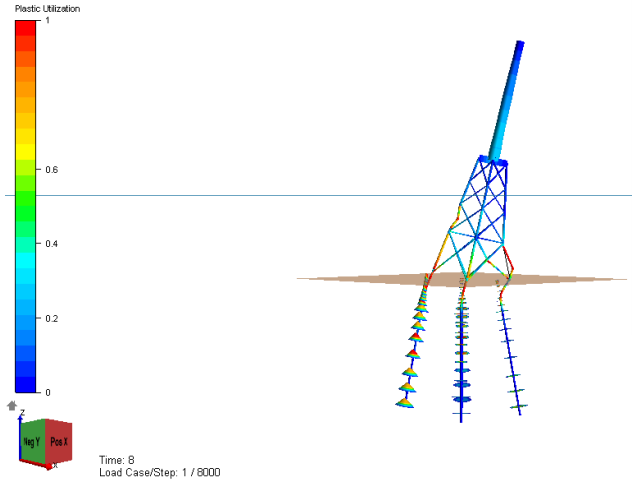


Dynamic plastic utilization for loaded ship column impact

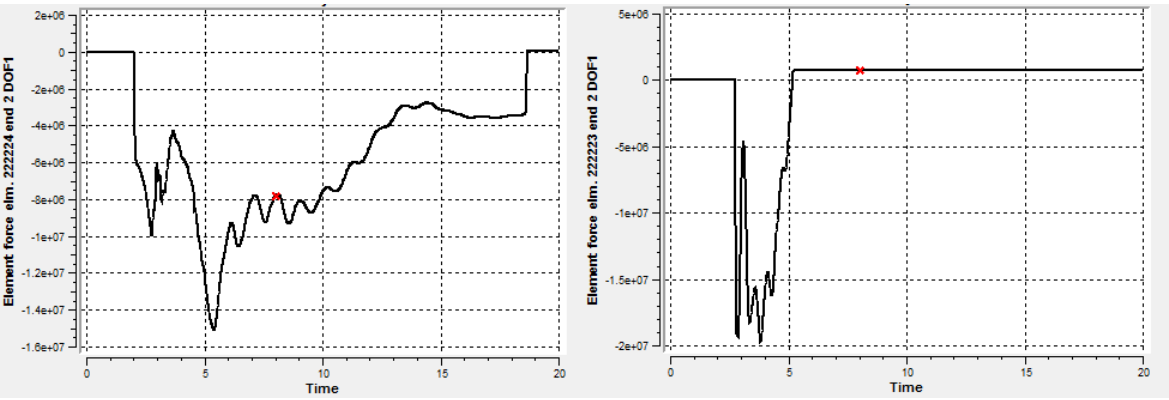


Dynamic spring forces for loaded ship column impact

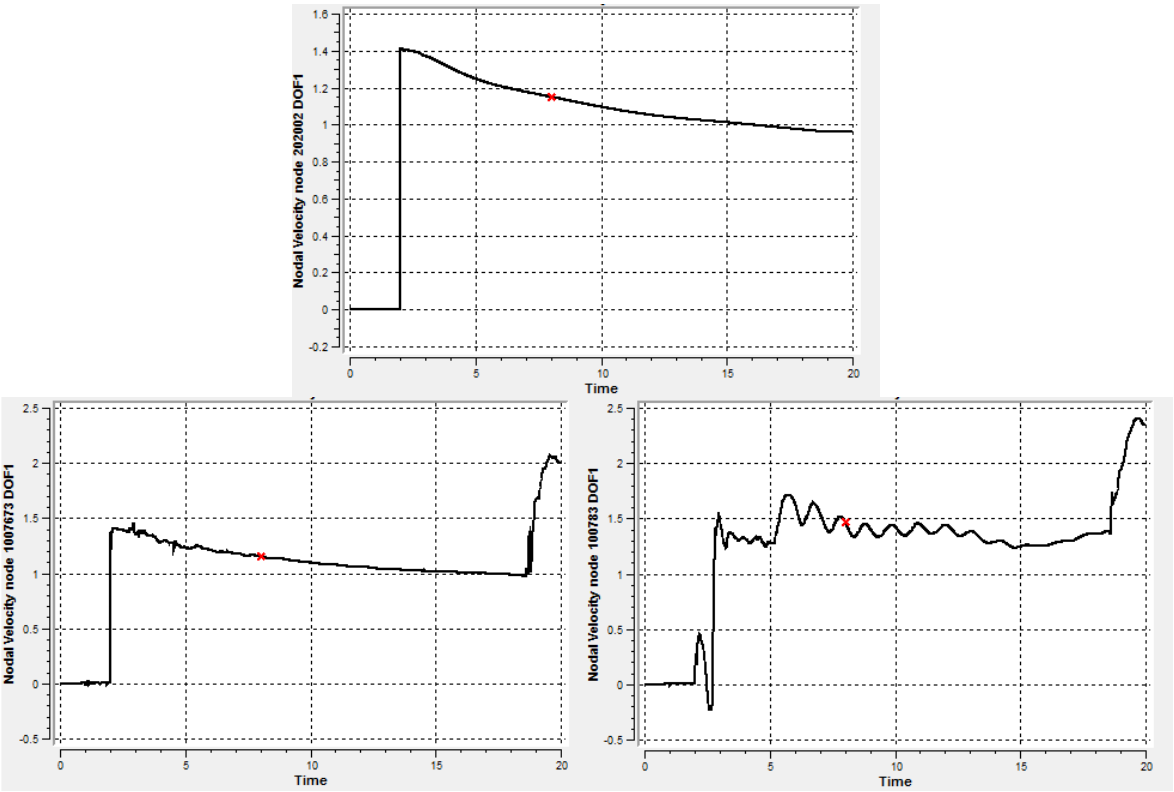


Dynamic ship velocity and velocity in impact node for loaded ship column impact

## B. CD

- Excel working sheets
    - Node interpolation
    - Operational offshore wind turbines in Europe, end 2010
    - Shell theory of local buckling of tower
    - Spring stiffness
- USFOS input files
    - Virtual Prototyping files
        - Dynamic analysis head file: head_dyn
        - Eigenvalue analysis head file: head_eig
        - Static analysis head file: head_sta
        - Model file: model
        - Soil file: soil_1
    - Modified files
        - Static analyses
            - Eigenvalue analysis
                - Head file: head_eig
                - Model file: model_eig
                - Soil file soil_eig
            - Loaded ship joint impact
                - Head file: head_sta_loaded_ship_joint_impact
                - Model file: model_sta_loaded_ship_joint_impact
                - Soil file: soil_sta_loaded_ship_joint_impact
            - Ballast ship joint impact
                - Head file: head_sta_ballast_ship_joint_impact
                - Model file: model_sta_ballast_ship_joint_impact
                - Soil file: soil_sta_ballast_ship_joint_impact
            - Loaded ship column impact
                - Head file: head_sta_loaded_ship_column_impact
                - Model file: model_sta_loaded_ship_column_impact
                - Soil file soil_sta_loaded_ship_column_impact
        - Dynamic analyses
            - Loaded ship joint impact
                - Head file: head_dyn_loaded_ship_joint_impact
                - Model file: model_dyn_loaded_ship_joint_impact
                - Soil file: soil_dyn_loaded_ship_joint_impact
            - Ballast ship joint impact
                - Head file: head_dyn_ballast_ship_joint_impact
                - Model file: model_dyn_ballast_ship_joint_impact
                - Soil file: soil_dyn_ballast_ship_joint_impact
                - Shell analysis
                    - Head file: head_shell_ballast_ship_joint_impact
                    - Model file: model_shell_ballast_ship_joint_impact

        - Soil file:
          soil_shell_ballast_ship_joint_impact
    - Loaded ship column impact
        - Head file: head_dyn_loaded_ship_column_impact
        - Model file: model_dyn_loaded_ship_column_impact
        - Soil file soil_dyn_loaded_ship_column_impact
        - Shell analysis
            - Head file:
              head_shell_loaded_ship_column_impact
            - Model file:
              model_shell_loaded_ship_joint_impact
            - Soil file:
              soil_shell_loaded_ship_joint_impact
- Master Thesis Report Henriette Flathaug Ramberg